Study of the strength of stray magnetic field in the vicinity of a single phase capacitor motor

Shirima, Desidery M.D.

Award date:
1997

Awarding institution:
University of Dar Es Salaam
Electrical Engineering

NETHERLANDS ORGANIZATION FOR INTERNATIONAL COOPERATION

IN

HIGHER EDUCATION (NUFFIC)

JAN TINBERGEN SCHOLARSHIP PROGRAM

STUDY OF THE STRENGTH OF STRAY MAGNETIC FIELD IN THE VICINITY OF A SINGLE PHASE CAPACITOR MOTOR

By

Desidery M. D. Shirima

EINDHOVEN UNIVERSITY OF TECHNOLOGY

THE NETHERLANDS

March 1997

Supervisors:
Prof. Dr. Ir. A.J.A. Vandenput
Chairman
Section Electromechanics and Power Electronics (EMV)
Department of Electrical Engineering
Eindhoven University of Technology
The Netherlands

Prof. P.N. Materu
Dean
Faculty of Engineering
University of Dar es Salaam
Tanzania

Acknowledgement

The author wishes to acknowledge NUFFIC (Netherlands Organization for International Cooperation in Higher Education) for awarding a fellowship within the Jan Tinbergen scholarship program, which has made this study possible in two Universities in two highly industrialized countries in Europe.

It is a pleasure to acknowledge all those who contributed in one way or another at the University of Dar es Salaam, Tanzania; Catholic University Leuven, Belgium and Eindhoven University of Technology, The Netherlands. It is not possible to forget the kindness that was accorded to this project and the author, in the three countries mentioned above.

I would like to express my sincere thanks to all members of the Section Electromechanical and Power Electronics at the Eindhoven University of Technology: the scientific staff, the technical staff, the research students and the secretariat for constant encouragement in my undertakings and advice for best results.

Special thanks to Prof. R. Belmans, Head of the Electrical Energy Research Group at the Catholic University Leuven, who made the finite element study and magnetic field measurement possible by allowing full cooperation of two senior Ph.D. students: Dipl. Ir. Uwe Pahner and Engineer Pieter van Roy. I really appreciate their exceptional kindness and assistance throughout my study. I must say that I am proud for the attention I had from all members of the group.

Last, but not least, I thank Prof. André J.A. Vandenput for his personal attention and advice from the beginning to the end of the study. His advice and previous work on capacitor induction motors will contribute significantly in my research at the university of Dar es Salaam and future practice in electrical machines.

Finally, I would like to thank Mr. J.C.v. Cranenbroek, the Head of CICA and his staff at Eindhoven University of Technology for the attention and the efficient coordination of all my activities in The Netherlands and Belgium, which is one of the secrets of my success.

ABSTRACT

The magnetic flux density distribution inside and outside a capacitor single phase induction motor has been studied.

The flux density around the motor has been calculated with the aid of finite element analysis. The actual magnetic flux density for a 1 kW, 220 V, 50 c/s, 2 pole capacitor induction motor was measured using an extra low frequency survey meter, HI-3604.

The flux density inside a 1.1 kW, 240 V, 50 c/s, 2 pole capacitor motor was also analyzed using two different finite element software programs. This motor was also simulated to observe the flux variations inside the motor both in transient and steady state conditions.

The results of the magnitude of the flux density around the motor known as stray field, obtained by finite element analysis and by practical measurement agree well at small distances from the motor.

The stray field around the motor is compared with the maximum allowable exposure level according to CENELEC Prestandard (European Committee for Electrotechnical Standards). The field very close to the motor exceeds the maximum allowable exposure to human beings.

STUDY OF THE STRENGTH OF STRAY MAGNETIC FIELD IN THE VICINITY OF A SINGLE PHASE CAPACITOR MOTOR

1 INTRODUCTION

1.1 GENERAL

There is a mounting evidence, that living organisms including human beings, are affected by electromagnetic fields [Sheppard, 1977; Konig, 1981; Polk, 1986; Smith & Best, 1989]. The nature of the effects depends on the subject, the medium through which the field travels from the source to the subject, the strength and the nature of the waveform and cumulative history of the field among others. Irrespective of the inadequacies in the existing data base, a survey of the extant literature indicates that several aspects of the biochemistry and physiology of cells and organized tissues may be perturbed by exposure to time varying extra low frequency (ELF) magnetic fields. ELF fields cover all frequencies above zero to 300 Hz. Konig summarized the reported biological effects from more than a hundred papers and these included:

1. Decreased rate of cellular respiration
2. Altered metabolism
3. Endocrine changes and altered hormonal responses of cells and tissues
4. Decreased cellular growth rate
5. Teratology and developmental effects
6. Morphological tissue changes in adult animals, frequently reversible after reversible exposure
7. Altered immune response to various antigens and lectines.

The single phase induction motor (SPIM) of the capacitor type, is the dominant prime mover in domestic applications [Veinott, 1948]. The domestic appliances here are such equipments as fridges, freezers, washing machines, vacuum cleaners, domestic food processors, air conditioners, hair driers, table fans, and many others. In today's civilized world, one can not live without these machines. The standard of living today is also associated with how such machines are used in a household [Chilikin, 1978; Rosenberg, 1970].

The SPIM has two main parts: the stationary part and a rotating part as shown in Fig. 1.1. The stator core and the stator coils are the stationary parts. The rotor core and the rotor windings are the rotating parts. In a capacitor motor, a capacitor is connected in series with one of the two stator coils to aid it during starting and/or improve its operating characteristics while running.

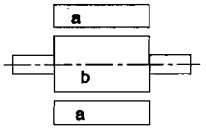

Fig. 1.1 Electric motor main parts

a) stator
b) rotor

The rotor is rotating due to the interaction of the magnetic fields of the stator and rotor currents. The rotor currents, however, are induced by time and space variations of the field originating from the stator coils. Not all the fields from the stator cross the air gap to the rotor. Some is lost as stray fields in the inside and outside of the motor. This phenomenon alone makes the SPIM a potential source of magnetic fields in space.

With the growing awareness of environmental protection, it is justified to study the external and internal magnetic field distributions of machines and reduce the strength of the external component at the design stage. Reducing the external stray field is possible by selecting material and geometries for the magnetic parts and the housing such that, for a given power delivery, the stray fields are minimum at the accessible distances [Amalia, 1996; Hesselgren et al, 1996]. The amount of stray magnetic field from a SPIM induction motor, in general, is in the group of between 1 and 5 Gauss (1 Gauss = 10^{-4} T) [Sheppard, 1977]. This is about ten times the natural magnetism one can safely encounter and sample geophysical values can be found elsewhere [Malmivuo, 1995; Polk, 1981]. The maximum allowable magnetic field exposure by European standards, is 0.1mT (1 Gauss) [CENELEC, ENV 50166-1, 1995].

Induction motors are designed to work in the saturation region of the magnetic materials [Wright et al, 1976; Veinott, 1959; Belmans et al, 1994]. There are economic advantages. The amount of material used per unit power output is relatively small [Wright et al, 1976]. While the motor has inherent stray fields of the order of power frequency, operation in the saturation region results also in spurious fields, the third and fifth being the strongest [Ben-Dev et al, 1980]. When a motor works in the saturation region, there will be an abnormal increase of current in the motor for small changes of flux as the load is increased above normal. In the performance analysis it is normally assumed that the relationship between flux and current is linear. The resulting currents increase the intensity of the stray fields [Matsch, 1972]. Overload currents are at a maximum in a machine with the rotor at standstill, i.e., when a motor blocks due to excessive loading. This condition of higher currents is always possible in domestic appliances.

The capacitor is included in the capacitor single phase induction motor (SPIM), to make it self starting [Veinott, 1948]. Sometimes, a capacitor is also used to improve its operating characteristic and this type of motor is the dominant in households. The capacitor is normally connected in series with one of two windings, the so called the auxiliary winding. When a motor is switched on, the initial current is several times higher than the rated current for a short duration. High starting currents of short duration, could give pulsed magnetic fields as e.g. in MRI applications [Laycock, 1995]. These result in magnetic shocks to cells of living organisms. Apart from transient currents which is increased by the addition of the capacitor, there also exist harmonic currents which also increase stray fields among other effects [Veinott, 1959]. Their frequencies are within the ELF region [Buchanan, 1965].

The biological effects of extra low frequency fields have been studied extensively by several scientists worldwide. Most of them have reported possible relationship between observed effects and direct exposure [Smith & Best, 1989; Indira et al, 1989; Malmivuo, 1995; Amalia, 1996; Sikora et al, 1996]. In many cases, the effects are not for the good of human beings [Sheppard, 1977; IEEE Magnetic Field Task Force Report, 1991 & 1993]. In some cases, however, these fields are used for medical diagnostics and curing [Konig, 1981; Malmivuo, 1995]. Studies of patients with medically intractable epilepsy at Electromedica, Erlangen,

Germany, utilize the information from biomagnetic signals originating from parts of the brain, where seizures start [Knutsson et al, 1993]. This is a diagnostic application of extra low frequency magnetic field before brain surgery is performed.

In a background paper, which was a recommended citation of the US Congress Office of Technology Assessment, OTA, Indira and others [Indira et al, 1989] concluded that there is a relationship between exposure to ELF fields and biological effects. Scientists have, in most cases, been unable to come out with a conclusion of what amount is dangerous: In terms of frequency and intensity; the amount of exposure for an effect to be noticeable; the transient exposure and the field threshold [Indira et al, 1989]. It can only be emphasized that induced current density in human tissue due to magnetic or electrical fields should not exceed 10 mA/m^2 [CENELEC ENV/50166-1:1994].

As an example, the mobility of calcium ions in the blood is responsible for the transmission of electrical signals to command different requests in the respective parts of the body [Sheppard, 1977; Konig, 1981]. Calcium is sometimes referred to as the second messenger (message carrier) of the human body. It is most affected in its role to transfer electrical signals in the body. It controls cellular protein, regulates muscle contraction including heart beats and developmental processes, such as egg maturation and ovulation [Indira et al, 1989; Sheppard, 1977].

The endocrine system of the human body is also dependent on the mobility of calcium ions in the body including in the brain [Konig, 1981]. This is disturbed by external fields as Kolin used Lorentz's equation to explain it and experiments to prove it [Sheppard, 1977; Malmivuo, 1995]. Information flow in human tissues in all processes is done by electric and magnetic fields [Malmivuo, 1995].

Malmivuo used Maxwell equations to show the coexistence of electric and magnetic fields in the human tissue, when subjected to time varying magnetic and electric fields. It is the same principle that is applied for heart and brain disease diagnostics [Malmivuo, 1995]. Maxwell's equations tie time varying electric and magnetic fields together such that, whenever there is a time varying magnetic field, there is a time varying electric field caused by it and vice versa. Literature on the coexistence of electric and magnetic time varying fields can be obtained elsewhere [Malmivuo, 1995; Jin, 1993; Schwab, 1980]. This means the existence of spurious magnetic fields not only disturbs biomagnetic formations of body cells and tissues but also bioelectric conditions [Malmivuo, 1995]. Appendix 13 is dedicated to detail this section.

Man is also exposed to higher frequency electric and magnetic fields. Devices such as stereo head phones (about 1 kHz), TV sets (about 20 kHz), radio transmitters (about 1 MHz), CB radios (about 30 MHz), FM radio and TV transmitters (about 100 MHz) and microwave ovens (about 1 GHz) [Indira et al, 1989]. The capacitor motor, however, is characterized by ELF in contrast to the above mentioned devices [Buchanan, 1965].

1.2 LITERATURE REVIEW

Studies in stray fields is limited to optimizing efficiency and minimizing losses. Baraton and Hutizler, have studied the stray field associated with the hair drier [Baraton et al, 1995]. The

hair drier was the item studied. Another study is by Hesselgren and Luomi [Hesselgren et al, 1996] on a small electric motor for domestic appliance. The study of stray losses in electric machines is normally emphasized in order to increase machine efficiency and not necessarily to limit electromagnetic pollution in the immediate environment. There is a lot of literature on studies on stray fields in induction motors, but none has a direct formula for calculating it under any condition [Ho et al, 1995]. In their report, however, Ho and Fu reported a fairly accurate method of determining stray losses caused by harmonic fields in an induction motor using 2D-finite element method. It is also suggested that the stray losses are directly proportional to the square of the machine current [Smith, 1990].

It is assumed that stray losses in an induction motor account for about 1% to 3% of the input power, and in some cases it may be as high as 5% [Ho et al, 1995]. There is neither an accurate method of predicting stray losses in an induction motor nor a simulation test that can conclude the same. There are some empirical formulas, which a designer may use but the state of the art is that, one has to make an educated guess and judge from experience [Veinott, 1959; Ho, 1995]. Stray losses increase with load due to additional core and eddy current losses. The losses mentioned here are due to air gap leakage fluxes and high frequency pulsations [Alger, 1970].

It is not mentioned exactly where does the power or energy associated with stray fields go. It is assumed that it is lost as heat, establishment of stray fields, eddy current effects, noise etc. How much is for example lost as stray fields, is not yet known. [Matsch, 1972; Say, 1986]. There are reports of research studies to reduce the strength of the stray fields in a domestic small motor [Hesselgren et al, 1996]. The work by Amalia, [Amalia, 1996], will also give some light of the effectiveness of the stator housing in reducing the strength of stray fields in relation to its material and dimensions.

It is possible to analyze the fields more accurately by numerical methods, such as finite element method (FEM), [Jin, 1993; Kong, 1989; Schwab, 1988; Henneberger et al, 1994; Dawson et al, 1994]. Since there are scientific observations and findings, that electric and magnetic fields of extremely low frequencies (ELF), are present in living organisms, and casting suspicion that they might be disturbed when the subject is overexposed to manmade fields from technical facilities, such as, the capacitor induction motor, [Malmivuo 1995; Sheppard, 1977; Konig, 1981; Indira et al, 1989], it is recommended to analyze accurately the external field of the most common domestic motor as well as its inside field.

A 2D-method was proposed, for simplicity, but much more accurate results might come from a 3D-method. Two pole machines have longer end windings compared with others with the same power rating. The distance covered by the overhang is too wide for the stray fields to be neglected. The best way of reducing the stray fields to a negligible level, is to consider them at the earlier stages of the design.

1.3 DESIGN OF A CAPACITOR SINGLE PHASE INDUCTION MOTOR (SPIM)

A single phase induction motor does not have a self starting mechanism, i.e. it does not develop a starting torque [Vandenput, 1985]. Therefore these motors (SPIMs) are identified by the starting method used. In the case of the capacitor SPIM, the capacitor which is usually

connected in series with the auxiliary winding, provides the starting mechanism, hence the name [Veinott, 1948].

The capacitor SPIM has three groups. These are: capacitor start, where the capacitor is disconnected when the motor has attained speed; two value capacitor, where one capacitor is disconnected when the motor has attained speed; and permanent split capacitor, where one capacitor is used for starting and running [Vandenput, 1985]. The last one is the most popular, also called permanent split phase induction motor [Veionott, 1948].

There are many design techniques, using several empirical formulas and approximations. Application of any method depends on the experience of the designer [Still, 1954; Veinott, 1959; Veinott, 1972], but the use of the computer is the most suitable today. These facilities are available, it is cheaper and more economical and less time consuming [Veinott, 1948; Belmans et al, 1994]. The author used mainly existing empirical formulas [Nwodo et al, 1993; Sawhney, 1984; Say, 1958; Sibal, 1970] to develop the permanent split capacitor motor. Finite element methods were used to analyze the magnetic flux distribution inside and outside the motor.

1.3.1 Design analysis

Small induction motors are actually designed to satisfy a certain set of operation specifications. Several design references can be consulted, like the references of the previous paragraph, including manuals, data books, and handbooks [Veinott, 1959]. Analysis of the design at the first stage will inform the designer about the loss characteristics of the machine. The bill of materials, manufacturing techniques in the later stages and successful utilization of the motor is actually dictated by the design. Stray fields can best be controlled at the design stage by careful selection of slot and teeth geometries for the stator and the rotor. Literature on this subject can be found elsewhere [Hamatta & Heller, 1977; Veinott, 1959; Buchanan, 1965]. Various techniques can be tested to find out if stray fields can be reduced in the design stage. The material for the end covers can be selected such that stray fields from end windings can be prohibited [Amalia, 1996]. Amalia found that the strength of magnetic induction arond a conductor at power frequency is reduced with increase of the shielding material. In the case of an induction motor, the end covers save as magnetic screens as well as mechanical support for the bearings.

1.3.2 Performance analysis

The analysis of the SPIM can be done on the computer. Different methods are at the disposal to the designer: [Suhr 1952; Veinott, 1959; Veinott, 1977; Vandenput, 1985; Veltman et al, 1991; Shirkoohi, 1992; Muljadi et al, 1993; Arfa et al, 1996]. The motor can be studied in three different operation modes. These are in capacitor start mode, two value capacitor mode and permanent split phase mode. A fourth one can be added if it is assumed that there exists a short circuit in the capacitor, i.e. a split phase mode [Vandenput, 1985]. Such a condition can arise and it will take some time before the fault is discovered and rectified. A program was developed for the permanent capacitor split phase type of motor.

Analysis of SPIM reveals the existence of forward and backwards revolving fields in operation. They cancel one another at standstill. The strength of the backward field can only be brought to a negligible minimum by optimization.

The induction motor commonly used in domestic appliances is the capacitor induction motor. Theory and experiment have proved that this type of motor can provide an optimal operating condition (maximum efficiency and minimum backward rotating field) at only one slip value, i.e. at only one load point [Vandenput, 1985]. Under practical conditions, the load varies as a machine is operating. When this happens, the backward field also varies. This means even if the motor was optimized, at rated load, practical load variations will make backward rotating fields unavoidable. These will also be experienced outside the motor as stray fields. This in itself guarantees that the single phase capacitor motor is also a domestic source of a pulsating magnetic field, since the two fields rotate in opposite directions at the same speed [Veinott, 1948; Suhr, 1952; Trickey, 1957; Matsch, 1972].

Single phase induction motors operate in the saturation region even at no load carrying relatively high stator currents on load [Hasselgen et al, 1996]. Stray field losses are directly proportional to the square of the current [Smith, 1990]. Stray losses increase with saturation [Matsch 1972]. Saturation increase spurious fields due to harmonic distortion [Belmans et al, 1982]. These inherent characteristics of the single phase induction motor make it a possible cause of stray fields in its surrounding region.

1.4 STATEMENT OF RESEARCH PROBLEM

Stray fields are produced in a capacitor SPIM by virtue of its construction [Belmans et al, 1982] and operating characteristics. Their frequencies fall within the extra low frequency range (ELF) [Say, 1986]. Scientists worldwide have reported possible negative effects to living beings due to exposure to ELF fields [Sheppard, 1977; Konig, 1981; Sikora et al, 1996].

Accurate methods such as FEM, have been developed to predict the magnetic field in machines [Belmans et al, 1994]. Application of this method to predict the external stray fields, together with practical measurements, will assist designers of such machines to have an advance knowledge of the strength of resulting stray fields in the environment of application.

The exact magnetic flux pattern outside a machine is very difficult to predict, even with the most sophisticated tools of analysis. The factors and parameters involved are numerous [Hasselgen et al, 1996]

1.4.1 RESEARCH OBJECTIVES

The objectives of this research are summarized as follows:
a) To determine the existence and the strength of stray fields outside a permanent capacitor single phase induction motor;
b) To establish the distance, from a 1 kW, two pole single phase induction motor, at which the field has decayed to an acceptable level;
c) To determine the two above mentioned items both by finite element analysis and practical measurements and compare the results of the two methods;

d) In addition to obtaining the outside magnetic field results by finite element analysis, to derive the flux distribution inside the motor, i.e. the stator and the rotor. The results will contribute to an ongoing research on the development of a computer aided engineering approach for the design and analysis of single phase induction motors, at the University of Dar es Salaam, Tanzania.

CHAPTER TWO

2 APPLICATION OF FINITE ELEMENT ANALYSIS.

It is known that the performance characteristic of any electric machine is normally predicted by the equivalent circuit approach, sometimes with some adjustments of the circuit parameters to allow for saturation and temperature effects. This classical method gives information of the mechanical torque, current and voltage in the machine. More literature on this subject is available elsewhere [Veinott, 1959; Vandenput, 1985; Chalmers, 1991].

This method alone does neither give accurately the detailed magnetic flux distribution inside the machine, which is actually responsible for the power transmission, nor the power loss in the magnetic structure. With environmental awareness, in addition, it does not give an estimation of the strength of the magnetic field surrounding the motor. As stated already in section 1.2, the stray fields are still obtained empirically [Ho, 1994].

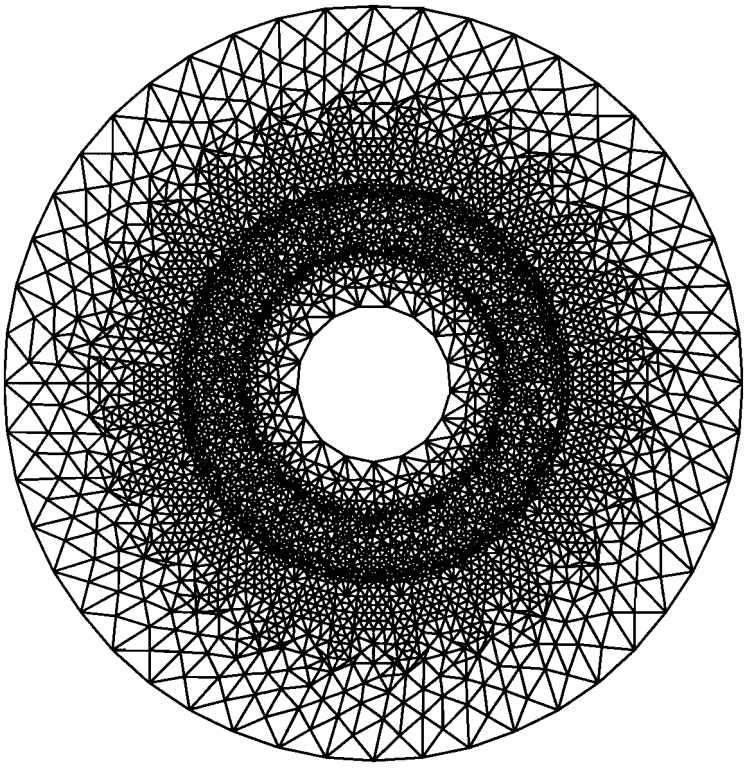

Fig. 2.1 Discretization of the region of analysis (meshing)

The area of magnetic influence is subdivided into regions i.e. discretized into finite elements, as shown in Fig. 2.1. This is generated automatically by the computer program and within each element the magnetic vector potential is obtained. The magnetic vector potential is assumed to have the unit of webers/meter. In simple terms, the flux that crosses between two known points with two different vector potentials would be the difference of the vector potentials at the two points in consideration divided by the distance between them. Literature on this subject is extensive and can be found elsewhere [Jin; J., 1993]. In a two dimensional analysis it is

assumed that the axial length of the region is infinite and it does not affect the end result. This is an approximation.

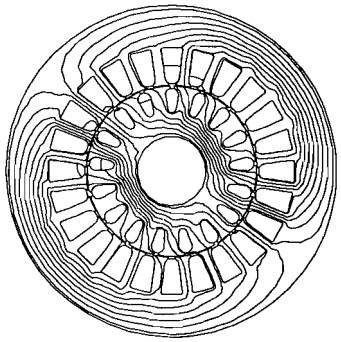

a) Equipotential lines of magnetic flux density due to current in the main winding

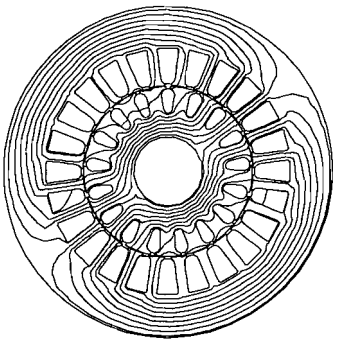

b) Equipotential lines of magnetic flux density due to the current in the auxiliary winding

Fig. 2.2 Equipotential lines in the stator and rotor of a capacitor single phase induction motor.

In a capacitor single phase induction motor there is a main winding and an auxiliary winding in the stator. The two windings are shifted by 90 degrees in space. Each winding contributes to the total field. The resultant field at any point is the vector sum of the two. In this literature, the real part is considered to be the field from the main winding and the imaginary part is considered to be the field from the auxiliary winding.

2.1 APPLICATION OF FINITE ELEMENT ANALYSIS TO MEASURE THE STRENGTH OF THE MAGNETIC FIELD AROUND A MOTOR 1.1 kW, 240 V., 50 C/S, 2860 RPM.

2.1.1 Use of Sisyphos electromagnetic solver

Sisyphos is a time harmonic electromagnetic solver which allows to include external circuits to the machine being analyzed. The capacitor is an external component in the single phase motor. The solver is available at the Catholic University of Leuven where the solution was obtained.

The equivalent end winding resistances and inductances of the stator windings and the rotor cage of the motor were first determined. The end winding resistance and inductance for the stator and rotor are treated as external components together with the capacitor. This is because they are neither directly connected with the distribution of flux within the machine nor production of mechanical forces in the electromechanical energy conversion. More literature on the treatment of end effects can be found elsewhere [Weerdt, 1995].

The geometry of the motor, characteristics of the material and external components were entered into the problem definition. A region of 110 cm radius was included for magnetic analysis. The outside radius of the stator core is 60 cm. This means the area of finite element analysis around the motor is 50 cm from the stator core periphery. This is based on the fact that the field around the motor decreases quickly as we move away from the motor [IEEE Magnetic Field Task Force, 1993; Polk, 1986]. The motor and the region were discretized as shown in Fig. 2.3

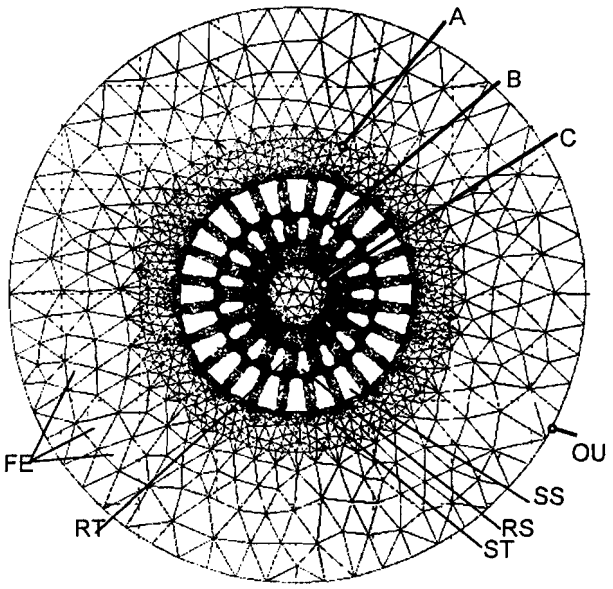

Fig. 2.3 Discretization of the region of magnetic analysis (mesh plot)

FE finite element
RT rotor tooth

ST	stator tooth
RS	rotor slot
SS	stator slot
OU	outside boundary
C	shaft/rotor boundary
B	rotor/stator boundary (the air gap)
A	stator boundary

The discretized (mesh) plot of the outside of the motor is shown in Fig. 2.4.

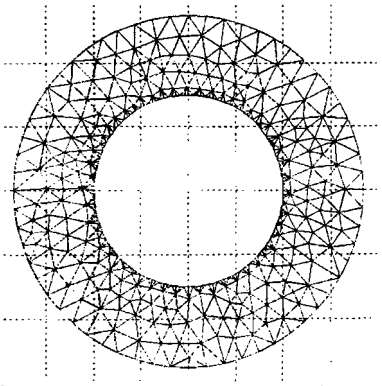

Fig. 2.4 Discretization of the outside region (motor parts excluded)

The resulting magnetic flux density distribution in the motor is shown in Fig. 2.5 and 2.6. The outside of the motor is detailed in Fig. 2.7 and Fig. 2.8. The flux density distribution for the outside can not be displayed simultaneously with the inside because of the wide difference in magnitude. To display and plot the outside equipotential lines, the motor itself has to be isolated as shown in Fig. 2.7 and Fig. 2.8.

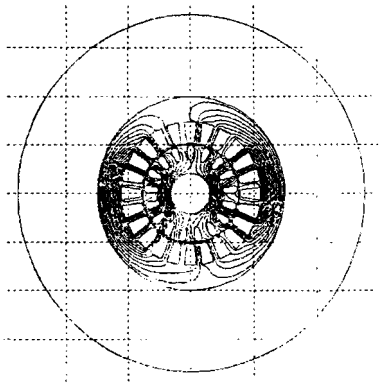

Fig.2.5 Equipotential lines (flux density due the main winding)

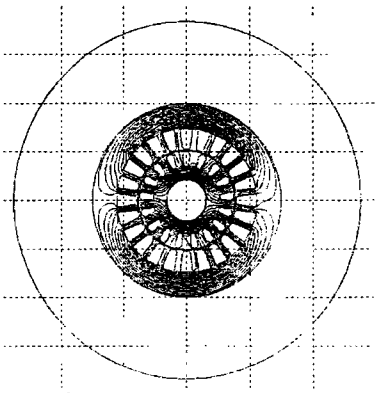

Fig. 2.6 Equipotential lines (flux due to the auxiliary winding)

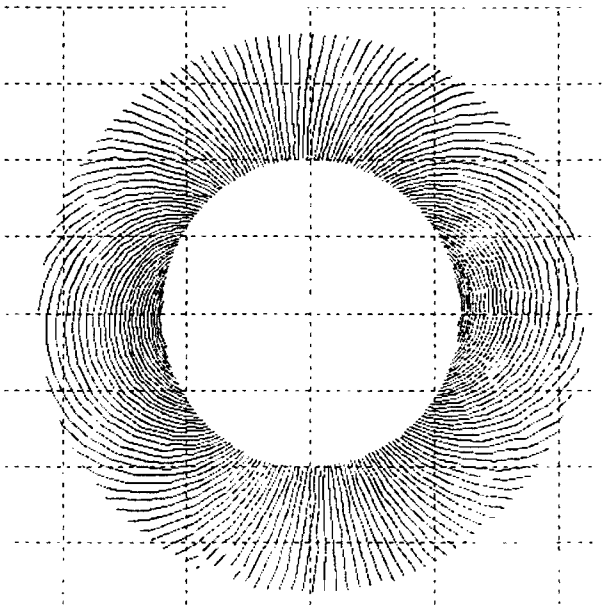

Fig. 2.7 Equipotential lines (outside only, flux density due to main winding)

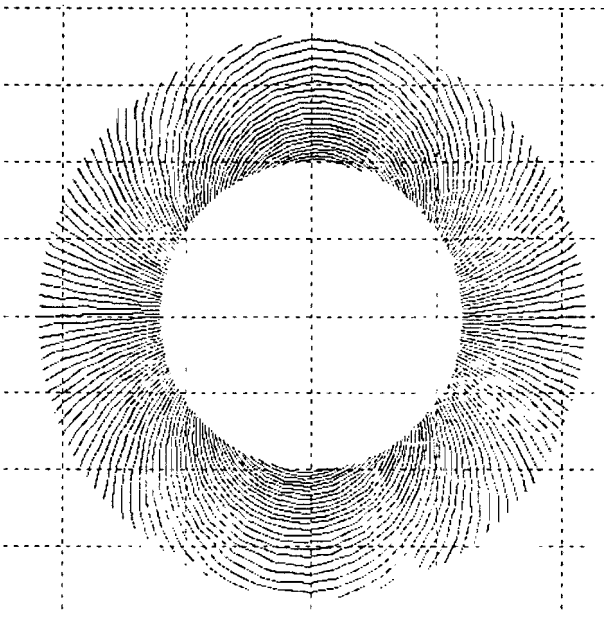

Fig. 2.8 Equipotential lines (flux density due to auxiliary winding, Outside only)

2.1.2 Calculation of flux density of the outside region of the motor using finite element results.

The effective flux density at any point in the region is the vector sum of the two fluxes, i.e. from Fig. 2.7 and Fig. 2.8. The two are read directly form the computer at different distances from the motor. The resultant scalar value is entered in table 2.1.

Table 2.1 Flux density around a capacitor single phase induction motor obtained by Finite Element Analysis

1.1 kW, 240 V, 50 c/s.					
Horizontal distance measured from the body housing					
Left			Right		
D[cm]	B[mT]	B est [mT]	D[cm]	B[mT]	B est [mT]
0.01	0.1619	0.165166	0.01	0.1612	0.162105
4	0.1619	0.148494	7	0.1612	0.132693
4	0.1529	0.148494	7	0.1236	0.132693
5	0.1529	0.14453	9	0.1236	0.12526
5	0.1388	0.14453	9	0.1042	0.12526
7	0.1388	0.13686	21	0.1042	0.08984
7	0.1172	0.13686	21	0.0886	0.08984
14	0.1172	0.112716	23	0.0886	0.085466
14	0.104	0.112716	23	0.0733	0.085466
25	0.104	0.083275	34	0.0733	0.069224
25	0.0794	0.083275	34	0.0656	0.069224
26	0.0794	0.081114	44	0.0656	0.065932
26	0.079	0.081114	44	0.0656	0.065932
27	0.079	0.079038			
27	0.0684	0.079038			
37	0.0684	0.063004			
37	0.0616	0.063004			
44	0.0616	0.056888			
44	0.0528	0.056888			
50	0.0528	0.054994			

The region between two successive vector potentials has a constant magnetic flux density. In the numeric method this is represented as steps. The actual value is the average value as shown in Fig. 2.9 and 2.10 as B est. B means the value of flux density on either side of the vector potential.

The graphs for the flux densities calculated to the left and right of the motor are plotted in Fig. 2.9 and 2.10 respectively. B is the flux density at two successive vector potentials. B est is the average flux density (to obtain a smooth curve).

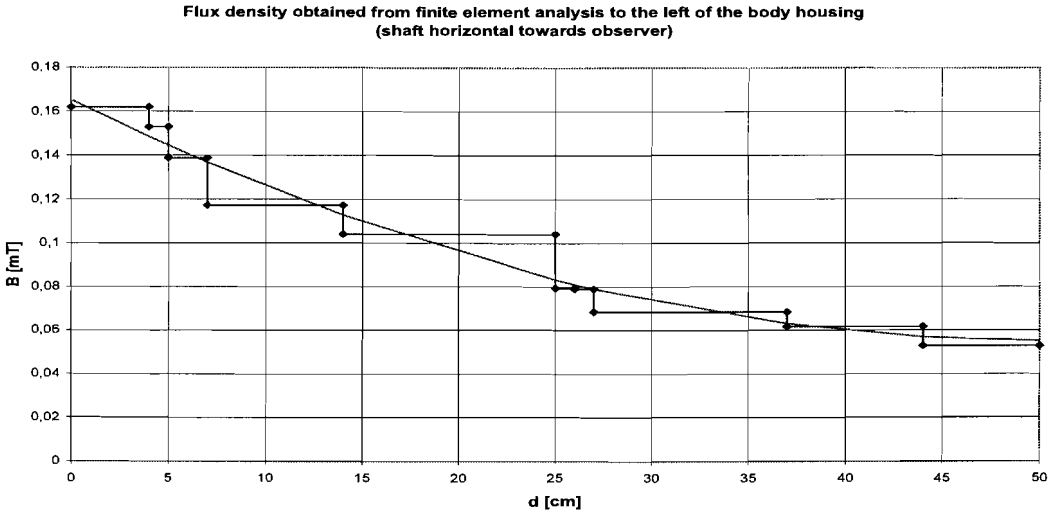

Fig. 2.9 Flux density calculated by using FEM to the left

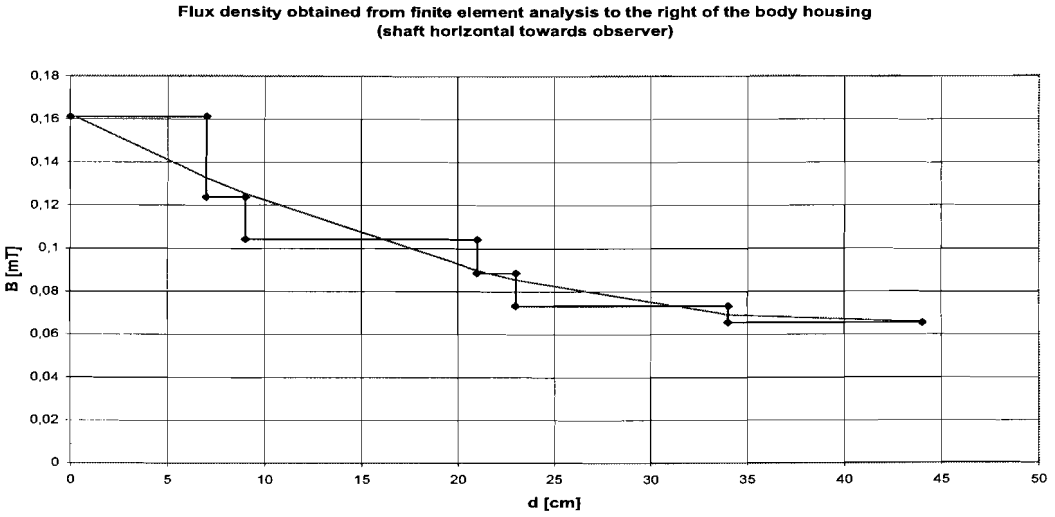

Fig. 2.10 Flux density calculated by FEM to the right of the motor

CHAPTER 3

3.1 Measurement of the stray magnetic field.

The stray field around a capacitor run type single phase induction motor was measured. The measurement was done in a screened high voltage laboratory at the Catholic University Leuven. A high voltage laboratory was selected because in such places the ambient magnetic field level is normally low; as low as 0.02 mG [IEEE Magnetic Field Task Force, 1991]. This motor was selected randomly. The ratings were 1000 W, 220 V, 10 A, 50 c/s, 2920 RPM, IP44, B3. The capacitance was 25 microfarad. Please note that the motor for the experiment slightly differs from the one used for finite element analysis.

The instrument used was an ELF Survey Meter, model HI-3604, Holaday Industries Inc. U.S.A. This is a power frequencyfield strength measuring instrument, designed to assist in the evaluation of magnetic and electric fields that are associated with 50/60 Hz electric power distribution and transmission lines along with electrically operated equipment and appliances. It has a direct digital readout of true RMS field strength, with facilities for external oscilloscope display. It can also display the maximum field strength during measurements.

The background magnetic field was observed to be between 0.165 mG to 0.185 mG. Initially a rough measurement was performed to establish an approximate relationship between the distance from the motor housing and the field strength measured. It was found that the field approaches the ambient value as the distance approaches 100 cm from the housing. Very little changes are recorded when the distance exceeds 50 cm. The distance in which the field variations were clearly noticeable was below 25 cm. from the housing.

The motor was running at no load with a current of 6.88 A. This value corresponds with the rated current of the motor analysed with the finite element [Arfa et al, 1996]. It is also within the requirements of the motor under development.

The magnetic field strength during starting of the motor was also recorded by following the instructions from the manual. The instrument measuring coil was held at a distance as prescribed and perpendicular to the plane being measured, i.e., for the vertical field, the instrument is held in the horizontal direction at the top.

The directions of measurement with respect to the motor are shown in Fig. 3.1 and Fig. 3.2. The load end means the motor side which the driven mechanical load is connected. The fan end is the motor side which a cooling fan is connected. In an ordinary motor the end windings are not symmetrically placed with respect to the load and fan end covers. These are a major source of external stray fields as they are normally hanging in the air inside the motor as shown in Fig. 3.3.

The results of the measurement of the magnetic field to the left, right and top of the motor are tabulated in Table 3.1. The results are plotted as follows: Fig. 3.4 flux density measured to the left of the motor; Fig. 3.5 flux density measured to the right

of the motor and Fig. 3.6 flux density measured at the top of the motor. The measured values are RMS values. In all the cases the contribution of the ambient magnetic field is relatively small in the region of interest. The maximum values were also recorded to assess the level of spikes mentioned in section 1.3.

The maximum values were plotted in the same graph for each direction.

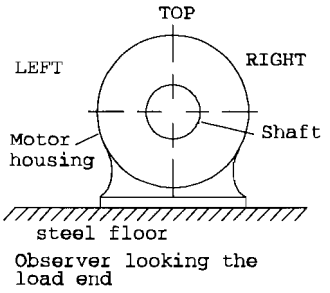

Fig. 3.1 Observer looking at the motor at the load end

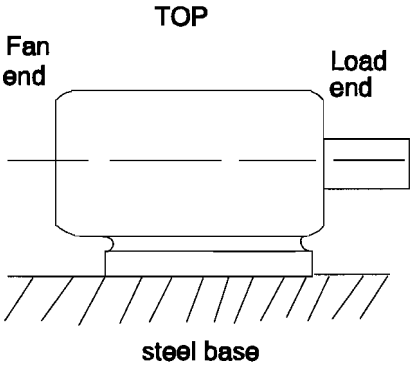

Fig. 3.2 Observer looking at the motor at both the load and fan end.

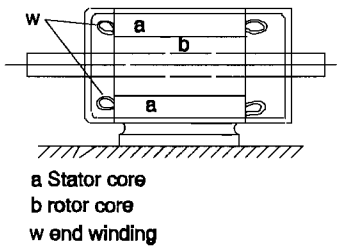

Fig. 3.3 Position of stator end windings in the motor

The flux density measured to the left of the motor is given in Fig. 3.4

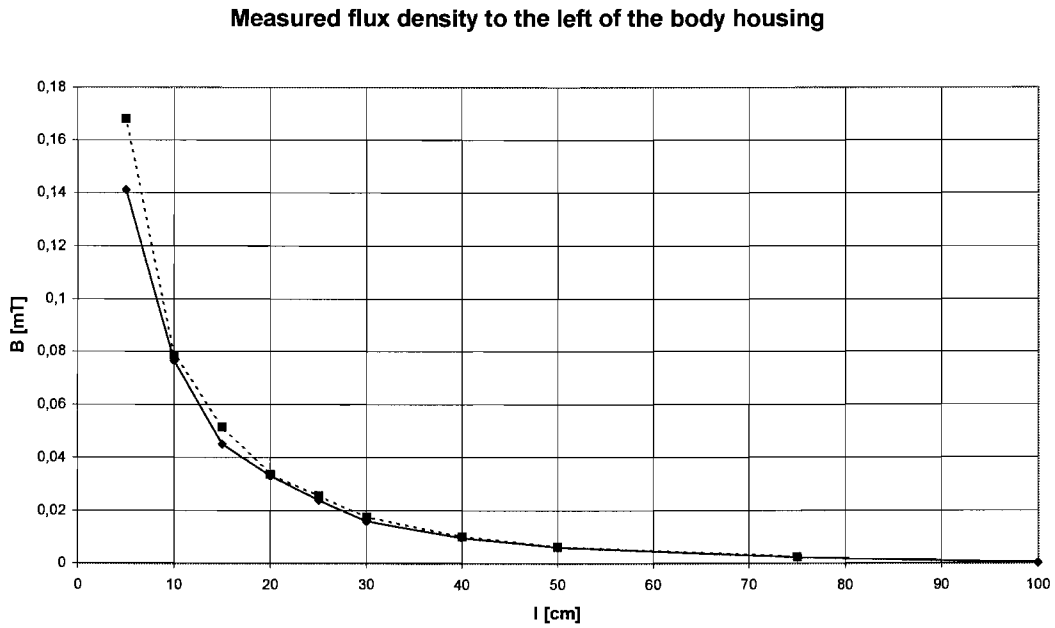

Fig. 3.4 Flux density measured to the left of the motor

The flux density measured at the top of the motor is shown in Fig. 3.6.

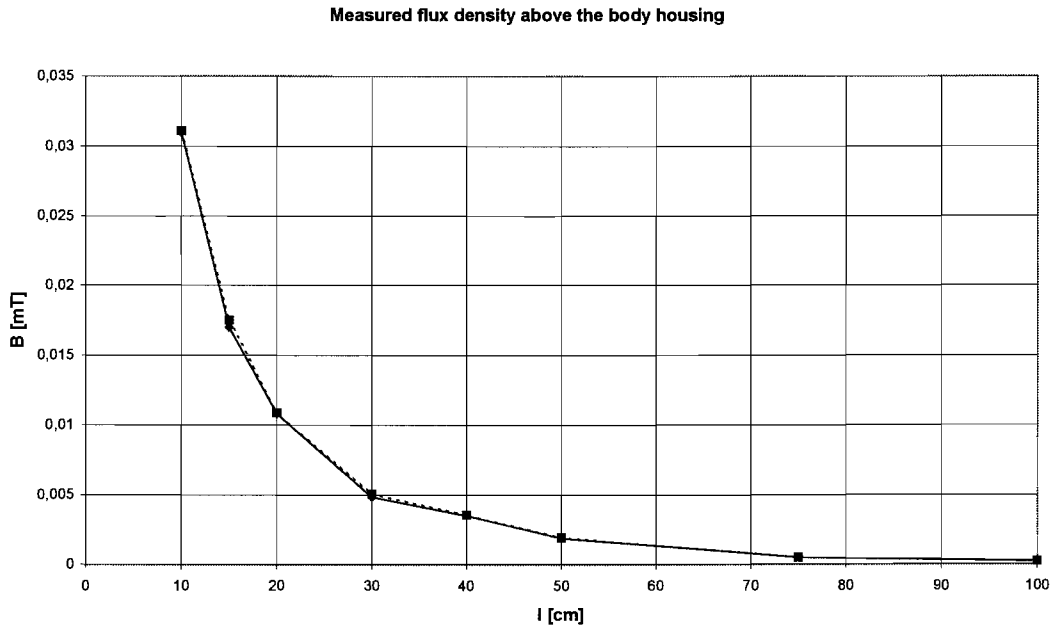

Fig. 3.6 Flux density measured at the top of the motor

CHAPTER 4

4 DISCUSSION OF THE RESULTS

4.1 Discussion of results obtained by finite element analysis

The accuracy of the results is limited to the solver ability to handle a case of a single phase motor. Solver Sisyphos can handle cases in which the rotating vectors have a constant magnitude. This is the case for three phase motors. In single phase motors the field is elliptical. The field can have a constant amplitude at only one load point, i.e. at the optimized load condition. Then, the resultant field across the air gap will have a circular pattern. Under practical conditions the load is not necessarily optimum. The air gap flux has an elliptical pattern. This means the circle tends to flatten. It increases in one axis while reducing in the other. The end result will be a modification of the flux density distribution pattern.

Sisyphos revealed some convergence problems. The values of flux density were read for the real part and the imaginary part and the resultant was calculated manually.

Magnet 5.2 software was used to study the flux distribution inside the motor. One limitation is that it could not solve the field problem inside the motor together with an external boundary around the motor to include the stray field analysis. Another limitation was that the rotor end winding impedance could not be included. This has made the rotor bars to be assumed short circuited. The results of the load and no-load condition are included in appendix 11 and 12 respectively.

Labels 1-24 correspond to the conductors in the stator slots. Labels 25-41 correspond to the rotor bars. Under optimized condition the equipotential plots for the main and auxiliary flux are displaced nearly 90 degrees as shown in Fig. 2.2.

The flux density around a contour at the center of the air gap obtained by using the Magnet software is shown in appendix 7. The flux density distribution in the stator and rotor teeth (at 1/3 distance from the air gap) are shown in appendix 8 and 9, respectively. Apart from being fundamental in electromechanical power conversion, these values are also responsible for teeth saturation and heating inside the motor.

The flux that travels to the outside environment of the motor crosses the stator back iron (the stator core). As the area external to the motor was not included in the analysis a flux distribution plot of a contour close to the outside periphery of the stator is shown in appendix 10. The flux is pulsating as predicted in section 1.1. The actual value that will reach a subject (a person exposed to) will depend on the material of the stator housing and the distance the subject will be from the motor housing.

4.2 Discussion of results obtained from measurement.

It was noted that the field is very pronounced in the load end and fan end region as predicted in chapter section 1.3.1. This is because of the end winding effect. The conductors in the stator slots are shielded by the stator core while the end windings are hanging in the air. The end covers of the motor studied were made of aluminum. The air in the motor and the end covers made of aluminum could not sufficiently block the flux from flowing outside. It is possible that eddy currents in the covers contribute to the outside field.

The values of the flux density were highest when the measuring instrument was held in the vertical plane to the x-axis if we assume a line from left to right crossing the load end in Fig. 3.1. This has a relation to the position of the windings in the motor. In general, this vertical plane had the highest readings.

The maximum values stored by the instrument while taking measurements were less than the transient values recorded when the motor is switched on. This corresponds to the theory that the starting currents are several times higher.

The motor under development was simulated by using a universal method for modelling electrical machines to observe the transient and steady state performance in relation to the magnetic field inside it [Veltman et al, 1991]. An optimized model was also used. The flux in the air gap was tracked by variation of the capacitor in the auxiliary winding for a load which is proportional to the square of the speed, such as a fan until it was circular. This is the optimum condition. The capacitance was found to be 25 microfarad. The dynamic response is shown in appendix 16. From the simulation it was justified that the flux has high values at the start and it varies with load. The pulsation effect also increases as the motor is away from the optimum condition. As long as the optimum condition can not be achieved in practical operations of the motor, then the statement that the motor is a potential source of spurious magnetic fields is true if they can cross to the outside.

4.3 CONCLUSION

There are stray fields outside a permanent capacitor induction motor. The strength of the field obtained by numerical method (Finite element method) and practical measurement agree well close to the housing.

Practical measurements in a 1 kW motor revealed that the field exceeds the CENELEC Prestandard level of 0.1 mT (1 Gauss), at a distance of about 7 cm or less to the left and 6 cm or less to the right. The maximum field in the top direction was less than 0.04 mT.

Further studies are recommended for various motors of different power outputs and number of poles to see if they are operating within the limits prescribed by the standards. In this respect it is also recommended to take stray fields outside the motor and their influence on human beings into account in the design stage.

References

1. Alger, P., Induction Machines: Their Behavior and Uses, Gordon & Breach Science Publishers, Inc., New York, 1970.
2. Amalia; I., "Shielding for Phase Conductors", *IEEE Transactions on Magnetics*, vol. 32, no. 3, pp. 1481-1484, 1996.
3. Arfa; K., Meziani; S., Hadji; S., Medjahed; B., "Modelization of Single Phase Capacitor Run Motors Accounting for Saturation", *International Conference of Electrical Machines*, pp. 113-118, 1996.
4. Baraton, P., Hutzler, B., "Magnetically induced currents in the human body", Electricite de France (EDF), IEC Technology Assessment Trend, France, 1995.
5. Belmans; R., Freeman, E., "Possibilities and Limitations of CAD-Finite Element Programs For Designing Electrical Machines". *Proceedings, International Conference on Electric Machines*, 1994
6. Ben-Dev, E., Harley, R.G., "Optimal Rating of a Given Load Diagram". *IEEE Transaction on Power Apparatus and Systems*, vol. PAS-80, no. 6, pp.2121-2127, 1980.
7. Chalmers; B.J., Williamson; A., A.C. Machines Electromagnetics and Design, Research Studies Press Ltd., Taunton, Somerset, England, 1991.
8. Buchanan; L.W., "Equivalent Circuit For a Single Phase Induction Motor Having Space Harmonics in its Magnetic Field", *IEEE Transactions on Power Apparatus and Systems*, vol. PAS-84, no. 11, pp. 993-999, 1984.
9. Chilikin, M., Electric Drive, Mir Publishers, Moscow, 1978.
10. Dawson, G., Freeman, E., Belmans, R., Filion, G., "A Re-evaluation of Induction Motor Analysis Methods", *2nd International Conference on Electric and Magnetic Fields From Numerical Methods to Industrial Applications*, Reports, Leuven, 1994.
11. CENELEC, European Prestandard, ENV 50166-1, "Human Exposure to Electromagnetic Fields, Low Frequencies (0-10 kHz), 1995.
12. Hasselgren; L., Luomi; J., "Reduction of External Magnetic Field Originating From a Small Electrical Motor", *International Conference on Electrical Machines*, pp. 423-428, 1996.
13. Henneberger, G., Schmitz, M., "Magnetic Field Analysis in Induction Motors in the Field Oriented Mode", *2nd International Conference on Electric and Magnetic Fields From Numerical Methods to Industrial Applications*, Reports, Leuven, 1994.
14. Ho, S.L., Fu, W.N., "Computation of Harmonic Stray Losses of Induction Motors Using Adaptive Time Stepping Finite Element Method Together With Externally Coupled Circuits", *International Conference on Electric Machines*, pp. 93-97, 1995.
15. Ho, S.L., "Study of Stray Losses Under Phantom Loading Conditions in Induction Motors", *International Conference on Electric Machines*, pp. 548-554, 1994.
16. IEEE Magnetic Field Task Force Report, "A Protocol For Spot Measurement of Residential Power Frequency Magnetic Fields", *IEEE Transactions on Power Delivery*, vol. 8, no. 3, pp. 1386-1394, 1993.
17. IEEE Magnetic Field Task Force Report, "An Evaluation of Instrumentation Used to Measure AC Power System Magnetic Fields", *IEEE Transactions on Power Delivery*, vol. 6, no. 1, pp. 373-383, 1991.
18. IEEE Magnetic Field Task Force, "Measurement of Power Frequency Magnetic Fields Away From Power Lines", *IEEE Transactions on Power Delivery*, vol. 6, no. 2, pp. 901-911, 1991.

19. Indira, N., Granger, M., Keith, H., "Biological Effects of Power frequency Electric and Magnetic Fields": Back ground paper, US Government Printing Office, Washington D.C., 1989.
20. Jin; J., The Finite Element Method in Electromagnetics, John Wiley & Sons, Inc., New york, 1993.
21. Knutsson; E., Hellstrand; E., Schneider; S., Striebel; W.," Multichannel Magnetoencephalography for Localization of Epileptogenic Activity in Intractable Epilepsies", *IEEE Transactions on magnetics*, vol. 29, no. 6, pp. 3321-3324, 1993.
22. Kong, J.A., Progress in Electromagnetic Research (PIER-4), Elsevier Science Publishing Co., Inc., New York, 1991.
23. Konig; H.L., Krueger; A.P., Lang; s., Sonning; W., Biological Effects of Environmental Magnetism, Springer-Verlag, New York, 1981.
24. Laycock; D.C., "Biological Effects of Natural and Pulsed Magnetic Fields", http://www.rscom.com/osteo/journal/ost1_3/vol_35.htm, 1995.
25. Malmivuo; Jaakko, Plonsey; Robert, Bioelectromagnetism: Principles and applications of bioelectric and biomagnetic fields, Oxford University Press, Inc., New York, 1995.
26. Matsch, L.W., Electromagnetic and Electromechanical Machines, 2nd. ed., IEP- A Dun Donnelley Publisher, New York, 1972.
27. Muljadi, E., Zhao, Y., Liu, T., Lipo, T.A., "Adjustable AC Capacitor For A Single Phase Induction Motor", *IEEE Transactions on Industry Applications*, vol. IAS-299, no. 3, pp. 479-484, 1993.
28. Nwodo, T.C., Ilochi, E.E., "Computer Aided Design and Construction of a Single Phase, 50 Hz. Fractional Horsepower Capacitor Start Induction Motor" *Conference Proceedings, Africa-USA International Conference on Manufacturing Technology*, Lagos, Nigeria, 1993.
29. Preston; T.W., Reece; A.B.J., "The Contribution of Finite Element Method to the Design of Electrical Machines: An Industrial Viewpoint", *IEEE Transactions on Magnetics*, vol. MAG-19, no. 6, pp. 2375-2380, 1983.
30. Polk; C., Postow; E., CRC Handbook of Biological Effects of Electromagnetic Fields, CRC Press, Inc., Boca Raton, Florida USA, 1986.
31. Rosenberg, R., Electric Motor Repair, 2nd ed., Holt, Rinehart and Winston, U.S.A., 1970.
32. Say, M.G., Alternating Current Machines, 5th ed., ELBS/Longman, London, 1986.
33. Say, M.G., Performance and Design of Alternating Current Machines, 3rd ed., Pitman Publishers, London, 1958.
34. Sawhney, A.K., A Course in Electric Machine Design, 5th ed., Dhanpat Rai & Sons, New Delhi, 1984.
35. Schawb; A.J., Field theory concepts, Springer-Verlag, New York, 1988.
36. Sibal, M.K., Electric Machine Design and Machine Drawing, Khana Publishers, New Delhi, 1970.
37. Sheppard; A.R., Eisemund; M., Biological Effects of Electric fields of Extremely Low Frequency, New York University Press, New York, 1977.
38. Shirkoohi, G.H., "Finite Element Solution of a Single Phase Induction Machine Cores Constructed From Anisotropic non-oriented Steels", *Journal of Magnetism and Magnetic Materials*, vol. 112, no. 1-3, pp. 451-453, 1992.
39. Sikora; R., Zenczack; M., "Electromagnetic Compatibility of Human organism and Medical Equipment Using Electrical Impedance Tomography", *8th International*

Symposium on Theoretical Electrical Engineering, pp. 286-289, 1995.

40. Smith; S., Best; C.W., Electromagnetic Man: Health and Hazard in the Electrical Environment, J.M. Dent & Sons Ltd., London, 1989.
41. Smith; A.C., White; I., Flem; Le G, Glew; C.N., "Frame Losses in Cage Induction Motors", *International Conference on Electrical Machines"*, pp. 405-410, 1996.
42. Suhr, F. W., "Towards Accurate Evaluation of Single Phase Induction Motor Constants", *AIEE Transactions on Power Apparatus and Systems*, vol. 71 Part III, pp. 221-227, 1952.
43. Still, A., Siskind, C., Elements of Electric Machine Design, 3rd ed., McGraw-Hill Book Company, New York, 1954.
44. Trickey, P.H., "Capacitor Motor Performance Calculations" *AIEE Transactions on Power Apparatus and Systems*, PAS Pt. III, vol. 75, pp. 1547-1553, 1957.
45. Wright; A., Little; G., "Numerical Determination of the Effects Magnetic Saturation of Induction Motors". *International Conference on Numerical Methods in Electrical and Magnetic Field Problems*, Conference Series, no. 1/76, International Centre For Computer Aided Design (ICCAD), 1976.
46. Vandenput; A.J.A., "Design and Run Capacitor Optimization of Single Phase Induction Motors", Ph.D. Thesis, University of Leuven, 1985.
47. Veinott, C.G., "Performance Calculation on Two Speed Shunted Capacitor Motor". *IEEE Transactions on Power Apparatus and Systems,* Vol. PAS-96, No. 4, pp. 1132-1141, 1977.
48. Veinott; C.G., Computer Aided Design of Electrical Machinery, Massechussets Institute of Technology Press, Massechussets, 1972.
49. Veinott; C.G., Theory and Design of Small Induction Motors, McGraw-Hill Book Company, Inc., New York, 1959.
50. Veinott; C.G., Fractional Horsepower Electric Motors, McGraw-Hill Book Company, Inc., New York, 1948.
51. Veltman; A., van den Bosch; P.P.J., "A universal method of modelling of electrical machines', Proccedings, IEE, Electrical Machines and Drives, pp. 193-197, 1991.
52. Weerdt; R. De; Eindige elementen modellering van kooianker inductiemotoren, Ph.D. Thesis, Catholic University of Leuven, Leuven, 1995.

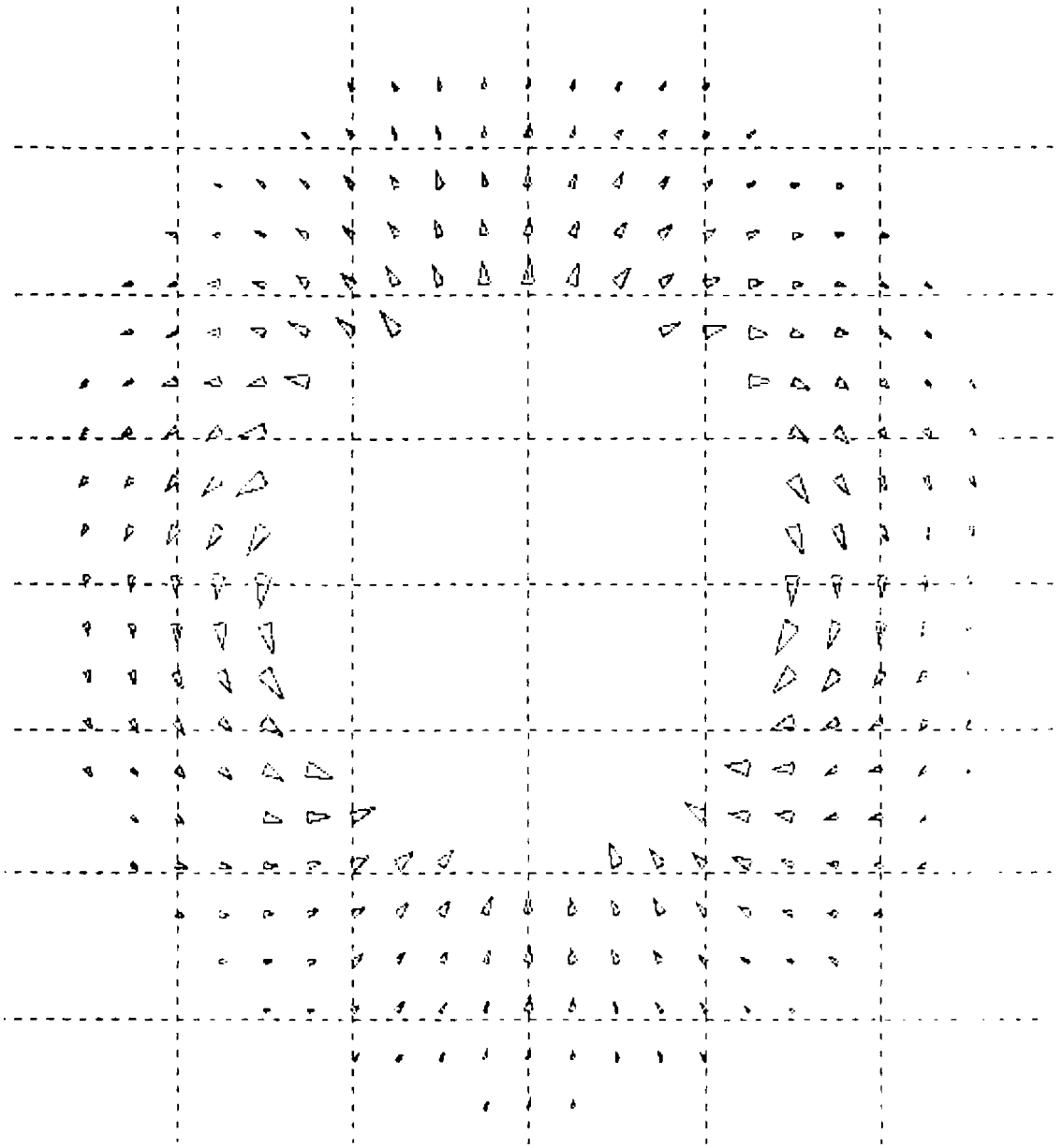

Appendix 1 Equipotential arrow plot of the magnetic field due to the main winding, surrounding a capacitor motor, 1.1 kW, 240 volts, 2 pole, 50 Hz, 25 microfarad.

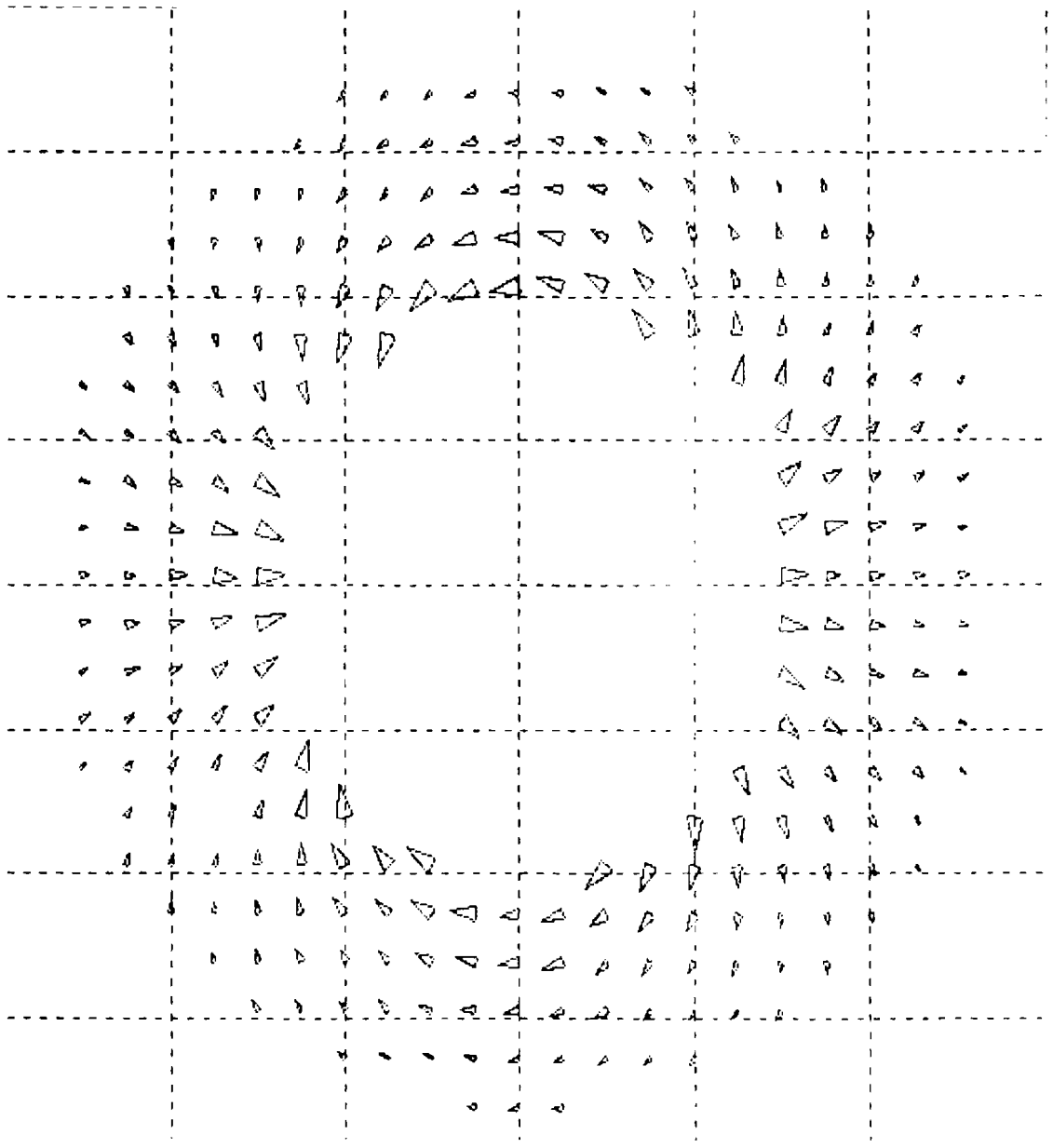

Appendix 2 Equipotential arrow plot of the magnetic field surrounding a capacitor single phase induction motor, 1.1 kW, 240 volts, 2 pole, 50 Hz, 25 microfarads on load.

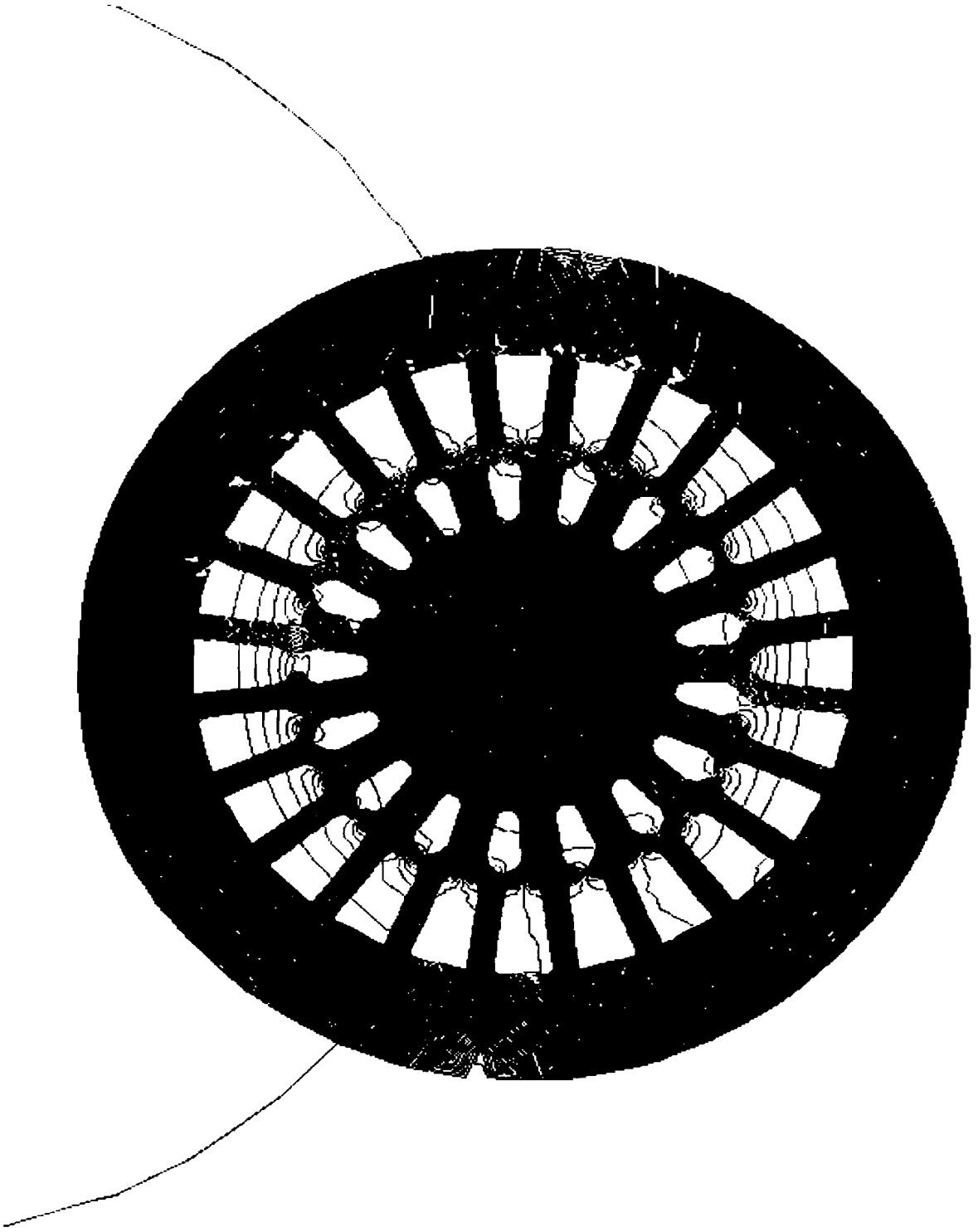

Appendix 3 Flux leakages inside a capacitor motor single phase induction motor, 1.1 kW, 240 volts, 2 pole, 50 Hz, due to the main winding

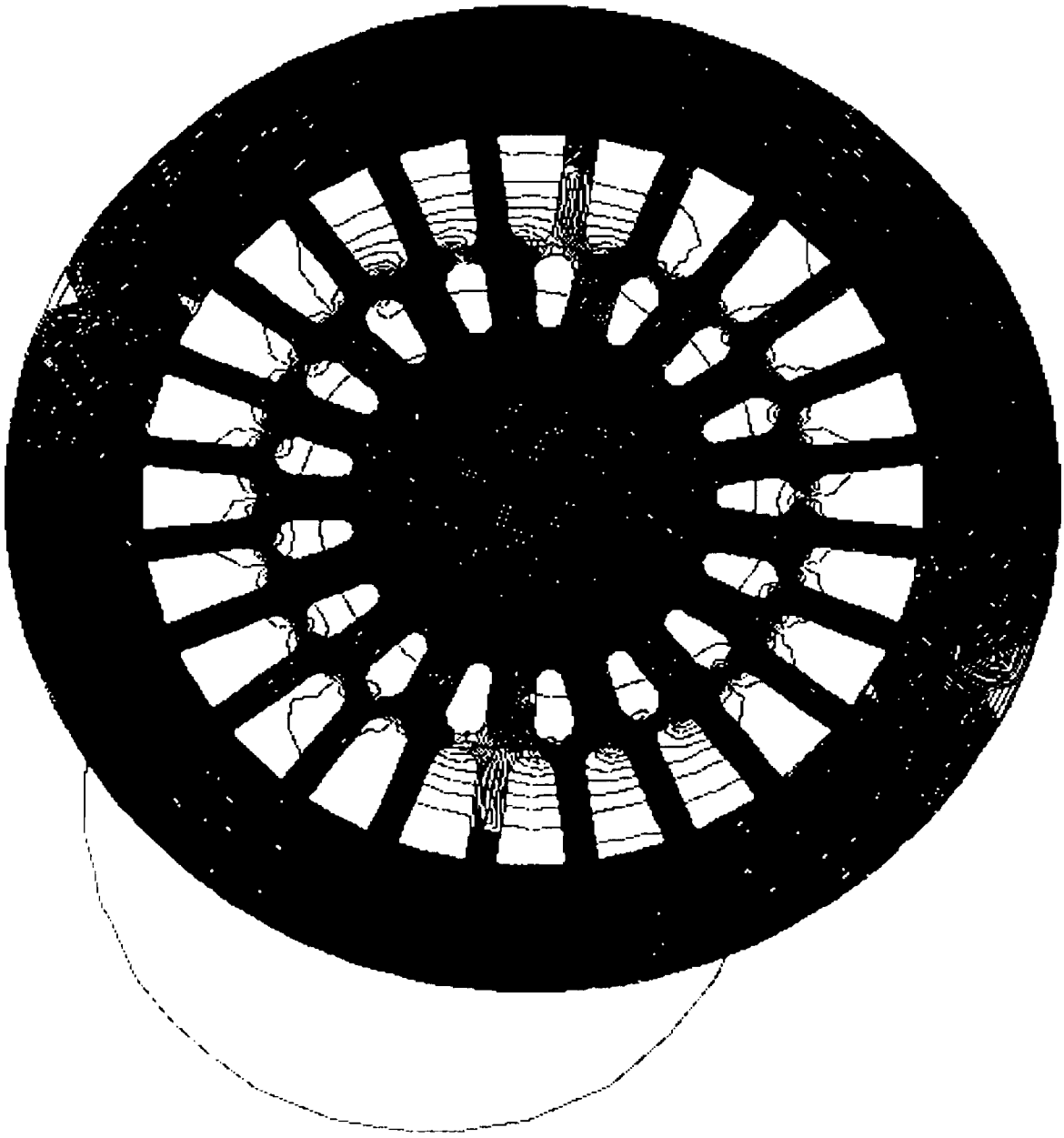

Appendix 4 Flux leakages inside a capacitor single phase induction motor 1.1 kW, 240 volts, 2 pole, 50 Hz, on load due to the auxiliary winding.

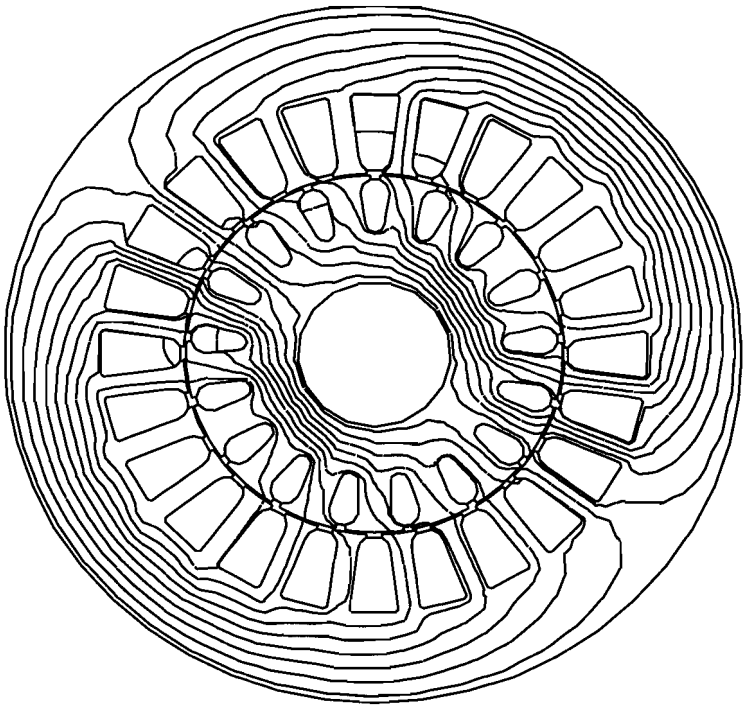

Appendix 5 Equipotential plot of the flux density inside a capacitor single phase induction motor, 1.1 kW, 240 volts, 50 Hz, on load due to the main winding.

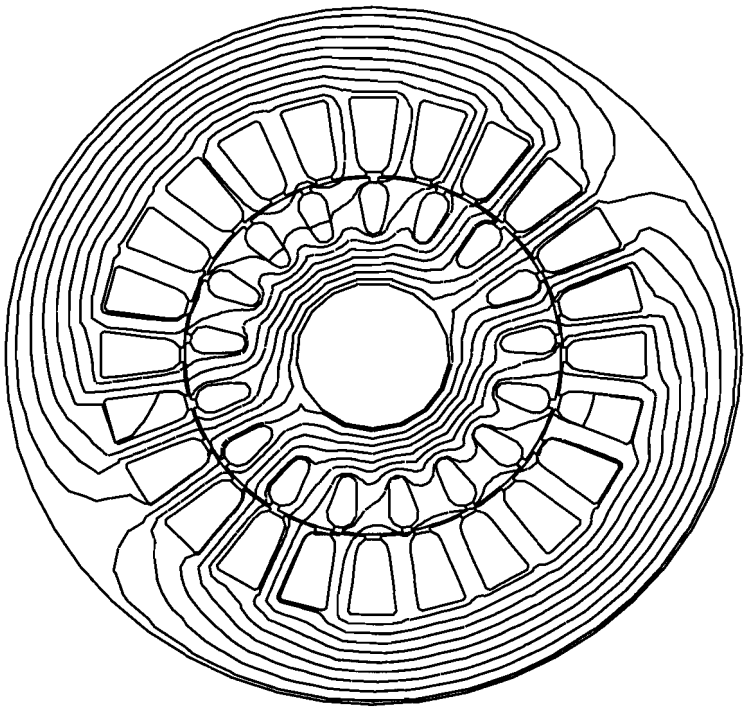

Appendix 6 Equipotential plot of a capacitor single phase induction motor, 1.1 kW, 240 volts, 2 pole, 50 Hz, due to the auxiliary winding.

Problem type: nominal load, first order, smoothed flux density

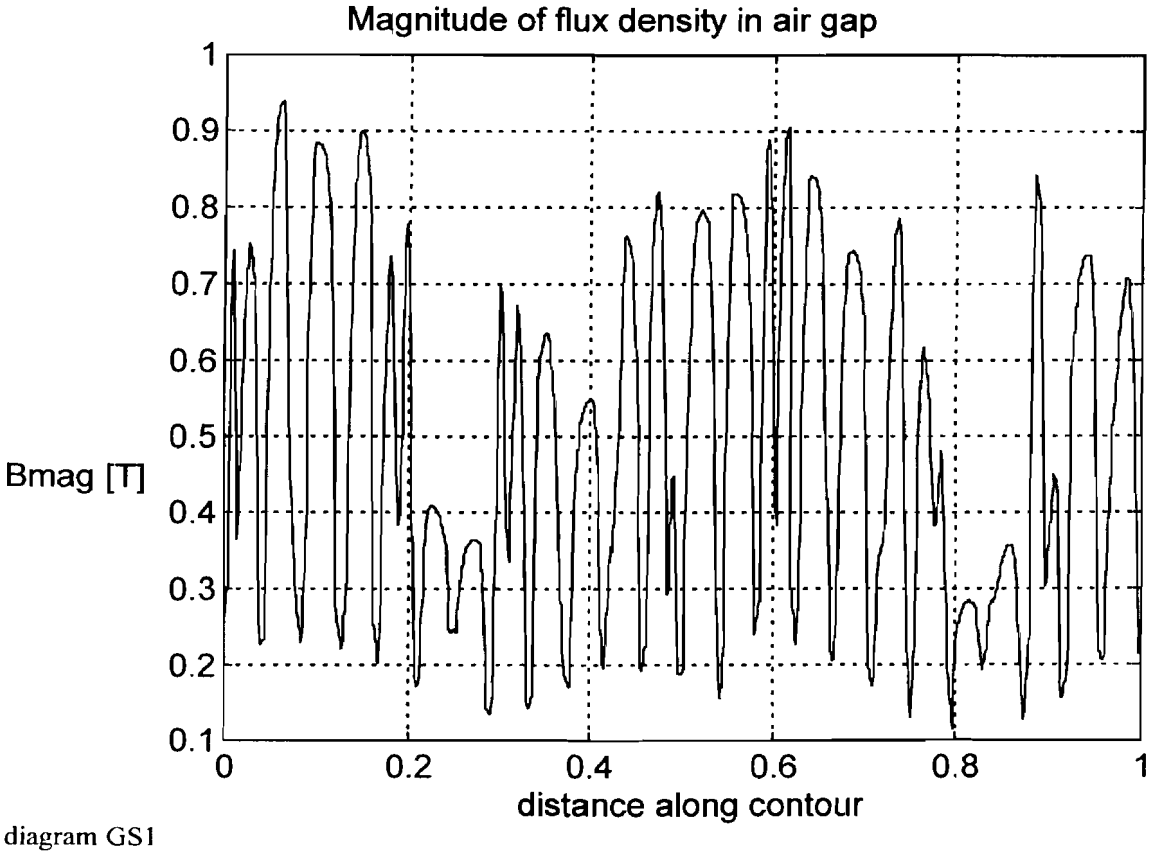

diagram GS1

Appendix 7 Magnitude of flux density at the centre of the air gap of a capacitor single phase induction motor 1.1 kW, 240 volts, 2 pole, 50 Hz, on load.

Appendix 8 Magnitude of flux density around a contour through all the stator teeth at 1/3 depth on load

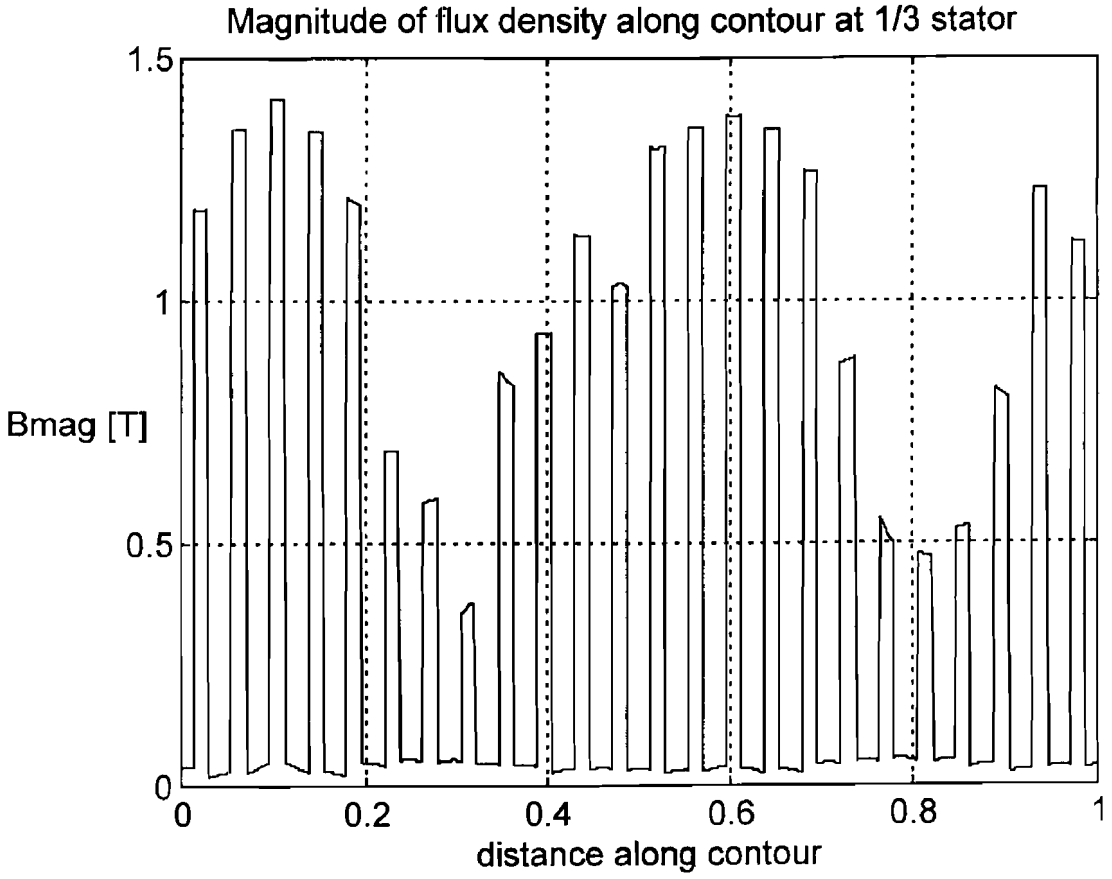

diagram GS3

Appendix 9 Magnitude of flux density around a contour through all the rotor teeth at 1/3 depth on load

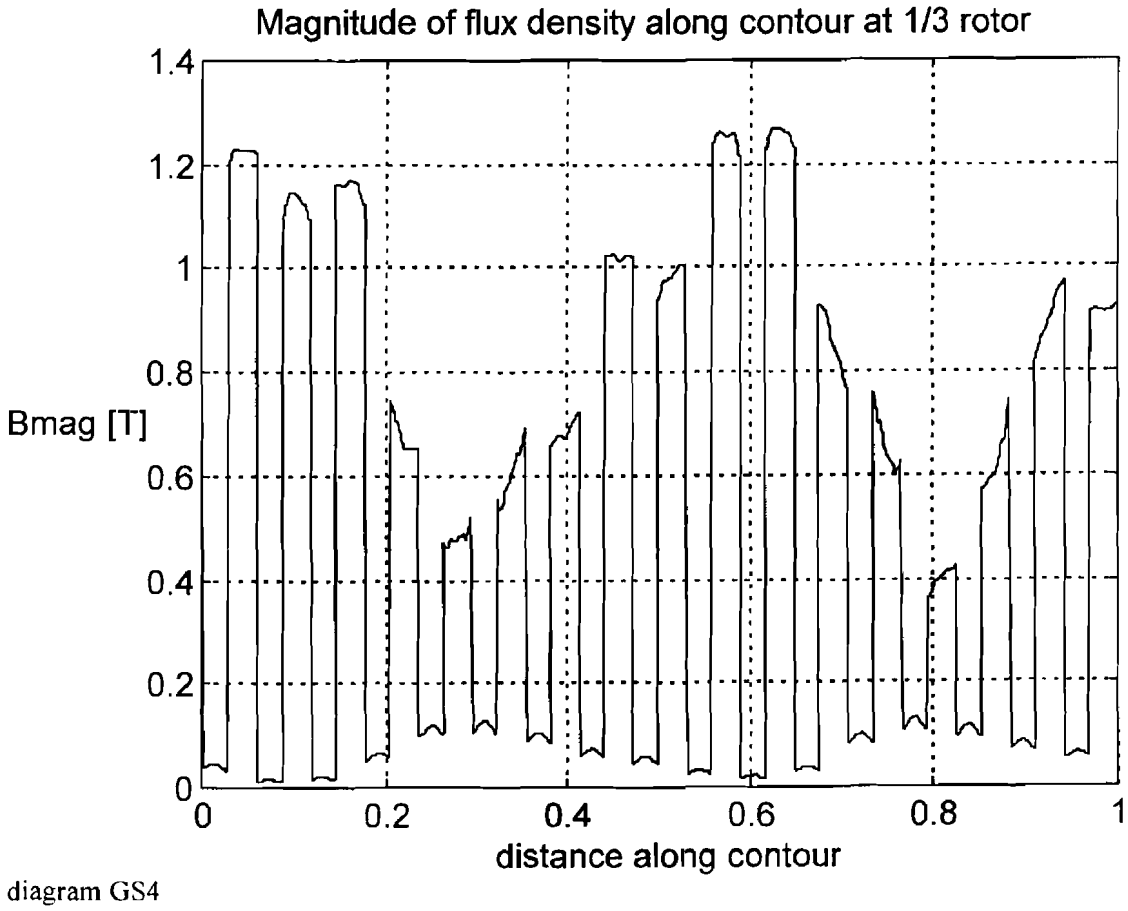

diagram GS4

Appendix 10 Magnitude of flux density around a contour near the stator core outside periphery on load.

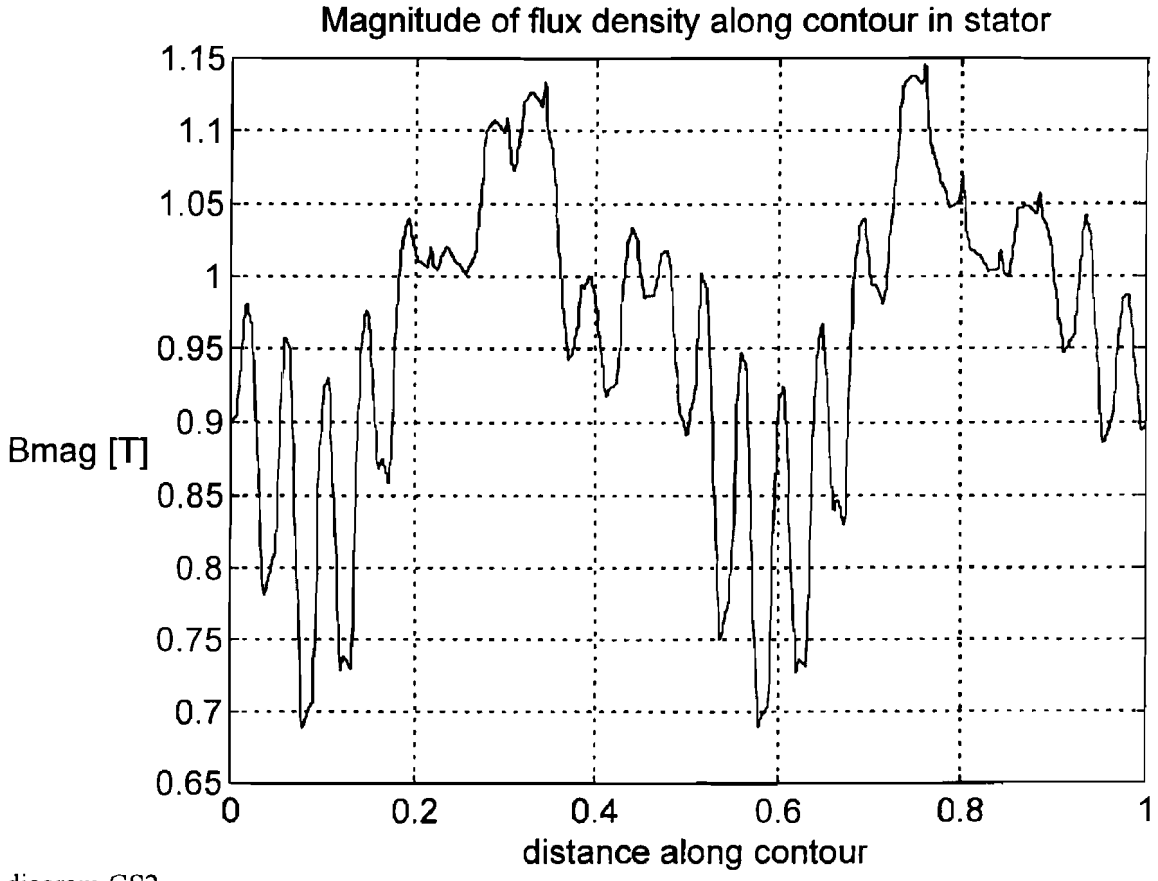

diagram GS2

Appendix 11 Load solution with Magnet 5.2

```
    ************************************************
    *
    *
    *                   TH2D
    *
    *           The MagNet 2D Eddy Current
    *            High Order (1-4) Solver
    *
    *                Release 5.2
    *
    *            Wed Jan 29, 1997  19:39
    *
    ************************************************
```

Maximum mesh size: 5120 nodes, 10240 elements
Number of problems filed for solution = 1
Problem names:
FMOT
The reordering of the mesh is in progress
Cartesian (xy) solution
Polynomial order 1
Completed pointer generation phase 1
Completed pointer generation phase 2
Completed pointer generation phase 3
Maximum number of field nodes in core = 5120
Maximum number of non-zeros in core = 33280
Number of field nodes = 3804
Number of non-zeros = 15151
Reading CIRCUIT.DAT

FMOT: TEST
Frequency: 5.0000E+01 Hz
Matrix Assembly
Manteuffel shift = .115
newton 1: 395 cg steps; change 100.000%, target .50%; time 0: 2:34
Matrix Assembly
Manteuffel shift = .115
newton 2: 143 cg steps; change 62.584%, target .50%; time 0:3:30
Matrix Assembly
Manteuffel shift = .115
newton 3: 196 cg steps; change 40.777%, target .50%; time 0:4:35
Matrix Assembly
Manteuffel shift = .115
newton 4: 255 cg steps; change 42.377%, target .50%; time 0:5:52
Matrix Assembly
Manteuffel shift = .115
newton 5: 302 cg steps; change 49.696%, target .50%; time 0:7:16

Matrix Assembly
Manteuffel shift = .115
newton 6: 309 cg steps; change 36.803%, target .50%; time 0:8:42
Matrix Assembly
Manteuffel shift = .115
newton 7: 287 cg steps; change 16.141%, target .50%; time 0:10:3
Matrix Assembly
Manteuffel shift = .115
newton 8: 277 cg steps; change 25.096%, target .50%; time 0:11:24
Matrix Assembly
Manteuffel shift = .115
newton 9: 220 cg steps; change 14.872%, target .50%; time 0:12:34
Matrix Assembly
Manteuffel shift = .115
newton 10: 267 cg steps; change 9.268%, target .50%; time 0:13:53
Matrix Assembly
Manteuffel shift = .115
newton 11: 219 cg steps; change 9.030%, target .50%; time 0:15:2
Matrix Assembly
Manteuffel shift = .115
newton 12: 255 cg steps; change 7.999%, target .50%; time 0:16:18
Matrix Assembly
Manteuffel shift = .115
newton 13: 212 cg steps; change 6.876%, target .50%; time 0:17:40
Matrix Assembly
Manteuffel shift = .115
newton 14: 244 cg steps; change 6.036%, target .50%; time 0:18:54
Matrix Assembly
Manteuffel shift = .115
newton 15: 205 cg steps; change 5.871%, target .50%; time 0:20:1
Matrix Assembly
Manteuffel shift = .115
newton 16: 223 cg steps; change 4.314%, target .50%; time 0:21:11
Matrix Assembly
Manteuffel shift = .115
newton 17: 204 cg steps; change 4.299%, target .50%; time 0:22:18
matrix Assembly
Manteuffel shift = .115
newton 18: 234 cg steps; change 4.046%, target .50%; time 0:23:31
Matrix Assembly
Manteuffel shift = .115
newton 19: 221 cg steps; change 4.209%, target .50%; time 0:24:41
Matrix Assembly
Manteuffel shift = .115
newton 20: 244 cg steps; change 3.879%, target .50%; time 0:25:55
Matrix Assembly
Manteuffel shift = .115
newton 21: 222 cg steps; change 4.010%, target .50%; time 0:27:5

Matrix Assembly
Manteuffel shift = .115
newton 22: 232 cg steps; change 3.755%, target .50%; time 0:28:21
Matrix Assembly
Manteuffel shift = .115
newton 23: 207 cg steps; change 3.798%, target .50%; time 0:29:32
Matrix Assembly
Manteuffel shift = .115
newton 24: 228 cg steps; change 3.596%, target .50%; time 0:30:47
Matrix Assembly
Manteuffel shift = .115
newton 25: 224 cg steps; change 3.679%, target .50%; time 0:31:57
Matrix Assembly
Manteuffel shift = .115
newton 26: 204 cg steps; change 3.504%, target .50%; time 0:33:4
Matrix Assembly
Manteuffel shift = .115
newton 27: 206 cg steps; change 3.500%, target .50%; time 0:34:12
Matrix Assembly
Manteuffel shift = .115
newton 28: 229 cg steps; change 3.404%, target .50%; time 0:35:23
Matrix Assembly
Manteuffel shift = .115
newton 29: 211 cg steps; change 3.438%, target .50%; time 0:36:31
Matrix Assembly
Manteuffel shift = .115
newton 30: 226 cg steps; change 3.374%, target .50%; time 0:37:42

Label 1, Conductivity: 4.6000E+07 S/m
Stranded conductor, 48 turn(s)
Area of strand: 7.9000E-07 sq.m.
DC Resistance: 1.0039E-01 Ohms
Current (rms): 6.9078E+00 Amps 1.1051E+02 degrees
Voltage (rms): 1.7388E+01 Volts -1.5964E+02 degrees
Time-avge. loss: 2.2426E+00 Watts

Label 2, Conductivity: 4.6000E+07 S/m
Stranded conductor, 45 turn(s)
Area of strand: 7.9000E-07 sq.m.
DC Resistance: 3.9001E+00 Ohms
Current (rms): 6.9078E+00 Amps 1.1051E+02 degrees
Voltage (rms): 2.8577E+01 Volts 1.4441E+02 degrees
Time-avge. loss: 8.1682E+01 Watts

Label 3, Conductivity: 4.6000E+07 S/m
Stranded conductor, 38 turn(s)
Area of strand: 7.9000E-07 sq. m.
DC Resistance: 3.2934E+00 Ohms

Current (rms): 6.9078E+00 Amps 1.1051E+02 degrees
Voltage (rms): 2.0407E+01 Volts 1.4109E+02 degrees
Time-avge. loss: 5.8246E+01 Watts

Label 4, Conductivity: 4.6000E+07 S/m
Stranded conductor, 29 turn(s)
Area of strand: 7.9000E-07 sq.m.
DC Resistance: 2.5134E+00 Ohms
Current (rms): 6.9078E+00 Amps 1.1051E+02 degrees
Voltage (rms): 1.2880E+01 Volts 1.3255E+02 degrees
Time-avge. loss: 3.3923E+01 Watts

Label 5, Conductivity: 4.6000E+07 S/m
Stranded conductor, 77 turn(s)
Area of strand: 3.9600E-07 sq.m.
DC Resistance: 3.2126E-01 Ohms
Current (rms): 2.9958E+00 Amps -1.1307E+02 degrees
Voltage (rms): 1.9490E+01 Volts -8.3314E+01 degrees
Time-avge. loss: 1.0854E+00 Watts

Label 6, Conductivity: 4.6000E+07 S/m
Stranded conductor, 83 turn(s)
Area of strand: 3.9600E-07 sq.m.
DC Resistance: 3.4629E-01 Ohms
Current (rms): 2.9958E+00 Amps -1.1307E+02 degrees
Voltage (rms): 2.3861E+01 Volts -5.9167E+01 degrees
Time-avge. loss: 1.2612E+00 Watts

Label 7, Conductivity: 4.6000E+07 S/m
Stranded conductor, 83 turn(s)
Area of strand: 3.9600E-07 sq.m.
DC Resistance: 3.4629E-01 Ohms
Current (rms): 2.9958E+00 Amps -1.1307E+02 degrees
Voltage (rms): 2.6469E+01 Volts -4.0703E+01 degrees
Time-avge. loss: 1.2612E+00 Watts

Label 8, Conductivity: 4.6000E+07 S/m
Stranded conductor, 77 turn(s)
Area of strand: 3.9600E-07 sq.m.
DC Resistance: 3.2126E-01 Ohms
Current (rms): 2.9958E+00 Amps -1.1307E+02 degrees
Voltage (rms): 2.4837E+01 Volts -2.3614E+01 degrees
Time-avge. loss: 1.0854E+00 Watts

Label 9, Conductivity: 4.6000E+07 S/m
Stranded conductor, 29 turn(s)
Area of strand: 7.9000E-07 sq.m.

DC Resistance: 6.0649E-02 Ohms
Current (rms): 6.9078E+00 Amps -6.9489E+01 degrees
Voltage (rms): 1.0225E+01 Volts -5.9630E+00 degrees
Time-avge. loss: 8.1858E-01 Watts

Label 10, Conductivity: 4.6000E+07 S/m
Stranded conductor, 38 turn(s)
Area of strand: 7.9000E-07 sq.m.
DC Resistance: 7.9472E-02 Ohms
Current (rms): 6.9078E+00 Amps -6.9489E+01 degrees
Voltage (rms): 1.4481E+01 Volts 3.8956E+00 degrees
Time-avge. loss: 1.4055E+00 Watts

Label 11, Conductivity: 4.6000E+07 S/m
Stranded conductor, 45 turn(s)
Area of strand: 7.9000E-07 sq. m.
DC Resistance: 9.4111E-02 Ohms
Current (rms): 6.9078E+00 Amps -6.9489E+01 degrees
Voltage (rms): 1.6444E+01 Volts 1.0375E+01 degrees
Time-avge. loss: 1.9710E+00 Watts

Label 12, Conductivity: 4.6000E+07 S/m
Stranded conductor, 48 turn(s)
Area of strand: 7.9000E-07 sq. m.
DC Resistance: 1.0039E-01 Ohms
Current (rms): 6.9078E+00 Amps -6.9489E+01 degrees
Voltage (rms): 1.8372E+01 Volts 1.5948E+01 degrees
Time-avge. loss: 2.2426E+00 Watts

Label 13, Conductivity: 4.6000E+07 S/m
Stranded conductor, 48 turn(s)
Area of strand: 7.9000E-07 sq. m.
DC Resistance: 1.0039E-01 Ohms
Current (rms): 6.9078E+00 Amps -6.9489E+01 degrees
Voltage (rms): 1.9732E+01 Volts 2.0803E+01 degrees
Time-avge. loss: 2.2426E+00 Watts

Label 14, Conductivity: 4.6000E+07 S/m
Stranded conductor, 45 turn(s)
Area of strand: 7.9000E-07 sq. m.
DC Resistance: 9.4111E-02 Ohms
Current (rms): 6.9078E+00 Amps -6.9489E+01 degrees
Voltage (rms): 1.5815E+01 Volts 2.7516E+01 degrees
Time-avge. loss: 1.9710E+00 Watts

Label 15, Conductivity: 4.6000E+07 S/m
Stranded conductor, 38 turn(s)
Area of strand: 7.9000E-07 sq. m.

DC Resistance: 7.9472E-02 Ohms
Current (rms): 6.9078E+00 Amps -6.9489E+01 degrees
Voltage (rms): 1.0931E+01 Volts 4.3421E+01 degrees
Time-avge. loss: 1.4055E+00 Watts

Label 16, Conductivity: 4.6000E+07 S/m
Stranded conductor, 29 turn(s)
Area of strand: 7.9000E-07 sq. m.
DC Resistance: 6.0649E-02 Ohms
Current (rms): 6.9078E+00 Amps -6.9489E+01 degrees
Voltage (rms): 6.8808E+00 Volts 6.6944E+01 degrees
Time-avge. loss: 8.1857E-01 Watts

Label 17, Conductivity: 4.6000E+07 S/m
Stranded conductor, 77 turn(s)
Area of strand: 3.9600E-07 sq. m.
DC Resistance: 3.2126E-01 Ohms
Current (rms): 2.9958E+00 Amps 6.6935E+01 degrees
Voltage (rms): 1.9303E+01 Volts 9.6654E+01 degrees
Time-avge. loss: 1.0854E+00 Watts

Label 18, Conductivity: 4.6000E+07 S/m
Stranded conductor, 83 turn(s)
Area of strand: 3.9600E-07 sq. m.
DC Resistance: 3.4629E-01 Ohms
Current (rms): 2.9958E+00 Amps 6.6935E+01 degrees
Voltage (rms): 2.3320E+01 Volts 1.2151E+02 degrees
Time-avge. loss: 1.2612E+00 Watts

Label 19, Conductivity: 4.6000E+07 S/m
Stranded conductor, 83 turn(s)
Area of strand: 3.9600E-07 sq. m.
DC Resistance: 3.4629E-01 Ohms
Current (rms): 2.9958E+00 Amps 6.6935E+01 degrees
Voltage (rms): 2.6799E+01 Volts 1.4153E+02 degrees
Time-avge. loss: 1.2612E+00 Watts

Label 20, Conductivity: 4.6000E+07 S/m
Stranded conductor, 77 turn(s)
Area of strand: 3.9600E-07 sq. m.
DC Resistance: 3.2126E-01 Ohms
Current (rms): 2.9958E+00 Amps 6.6935E+01 degrees
Voltage (rms): 2.7086E+01 Volts 1.5577E+02 degrees
Time-avge. loss: 1.0854E+00 Watts

Label 21, Conductivity: 4.6000E+07 S/m
Stranded conductor, 29 turn(s)
Area of strand: 7.9000E-07 sq. m.

DC Resistance: 6.0649E-02 Ohms
Current (rms): 6.9078E+00 Amps 1.1051E+02 degrees
Voltage (rms): 9.8233E+00 Volts 1.7159E+02 degrees
Time-avge. loss: 8.1858E-01 Watts

Label 22, Conductivity: 4.6000E+07 S/m
Stranded conductor, 38 turn(s)
Area of strand: 7.9000E-07 sq. m.
DC Resistance: 7.9472E-02 Ohms
Current (rms): 6.9078E+00 Amps 1.1051E+02 degrees
Voltage (rms): 1.3515E+01 Volts -1.7559E+02 degrees
Time-avge. loss: 1.4055E+00 Watts

Label 23, Conductivity: 4.6000E+07 S/m
Stranded conductor, 45 turn(s)
Area of strand: 7.9000E-07 sq. m.
DC Resistance: 9.4111E-02 Ohms
Current (rms): 6.9078E+00 Amps 1.1051E+02 degrees
Voltage (rms): 1.8398E+01 Volts -1.6851E+02 degrees
Time-avge. loss: 1.9710E+00 Watts

Label 24, Conductivity: 4.6000E+07 S/m
Stranded conductor, 48 turn(s)
Area of strand: 7.9000E-07 sq. m.
DC Resistance: 1.0039E-01 Ohms
Current (rms): 6.9078E+00 Amps 1.1051E+02 degrees
Voltage (rms): 1.9208E+01 Volts -1.6446E+02 degrees
Time-avge. loss: 2.2426E+00 Watts

Label 25, Conductivity: 1.1100E+06 S/m
DC Resistance: 2.1162E-03 Ohms
Current (rms): 3.5648E+01 Amps 1.2232E+01 degrees
Voltage (rms): 2.5478E-01 Volts -1.5448E+02 degrees
Time-avge. loss: 2.7137E+00 Watts

Label 26, Conductivity: 1.1100E+06 S/m
DC Resistance: 2.1162E-03 Ohms
Current (rms): 3.8350E+01 Amps 2.2721E+01 degrees
Voltage (rms): 2.2415E-01 Volts -1.3905E+02 degrees
Time-avge. loss: 3.1194E+00 Watts

Label 27, Conductivity: 1.1100E+06 S/m
DC Resistance: 2.1162E-03 Ohms
Current (rms): 2.9217E+01 Amps 6.2967E+01 degrees
Voltage (rms): 1.8596E-01 Volts -1.1319E+02 degrees
Time-avge. loss: 1.8071E+00 Watts

Label 28, Conductivity: 1.1100E+06 S/m

DC Resistance: 2.1162E-03 Ohms
Current (rms): 3.0820E+01 Amps 1.0103E+02 degrees
Voltage (rms): 1.7360E-01 Volts -7.8473E+01 degrees
Time-avge. loss: 2.0104E+00 Watts

Label 29, Conductivity: 1.1100E+06 S/m
DC Resistance: 2.1162E-03 Ohms
Current (rms): 4.0746E+01 Amps 1.3885E+02 degrees
Voltage (rms): 1.9679E-01 Volts -4.5526E+01 degrees
Time-avge. loss: 3.5163E+00 Watts

Label 30, Conductivity: 1.1100E+06 S/m
DC Resistance: 2.1162E-03 Ohms
Current (rms): 3.6217E+01 Amps 1.6076E+02 degrees
Voltage (rms): 2.2648E-01 Volts -2.1931E+01 degrees
Time-avge. loss: 2.7831E+00 Watts

Label 31, Conductivity: 1.1100E+06 S/m
DC Resistance: 2.1162E-03 Ohms
Current (rms): 3.1340E+01 Amps -1.6655E+02 degrees
Voltage (rms): 2.5048E-01 Volts -3.9356E+00 degrees
Time-avge. loss: 2.0905E+00 Watts

Label 32, Conductivity: 1.1100E+06 S/m
DC Resistance: 2.1162E-03 Ohms
Current (rms): 3.0928E+01 Amps -1.5706E+02 degrees
Voltage (rms): 2.6512E-01 Volts 9.0447E+00 degrees
Time-avge. loss: 2.0476E+00 Watts

Label 33, Conductivity: 1.1100E+06 S/m
DC Resistance: 2.1162E-03 Ohms
Current (rms): 3.3067E+01 Amps -1.6549E+02 degrees
Voltage (rms): 2.6351E-01 Volts 1.9598E+01 degrees
Time-avge. loss: 2.3427E+00 Watts

Label 34, Conductivity: 1.1100E+06 S/m
DC Resistance: 2.1162E-03 Ohms
Current (rms): 3.8458E+01 Amps -1.6421E+02 degrees
Voltage (rms): 2.4217E-01 Volts 3.1978E+01 degrees
Time-avge. loss: 3.1467E+00 Watts

Label 35, Conductivity: 1.1100E+06 S/m
DC Resistance: 2.1162E-03 Ohms
Current (rms): 3.6055E+01 Amps -1.4467E+02 degrees
Voltage (rms): 2.0386E-01 Volts 5.1490E+01 degrees
Time-avge. loss: 2.7529E+00 Watts

Label 36, Conductivity: 1.1100E+06 S/m

DC Resistance: 2.1162E-03 Ohms
Current (rms): 2.6422E+01 Amps -9.6460E+01 degrees
Voltage (rms): 1.7196E-01 Volts 8.3662E+01 degrees
Time-avge. loss: 1.4778E+00 Watts

Label 37, Conductivity: 1.1100E+06 S/m
DC Resistance: 2.1162E-03 Ohms
Current (rms): 3.8391E+01 Amps -5.3836E+01 degrees
Voltage (rms): 1.8261E-01 Volts 1.2010E+02 degrees
Time-avge. loss: 3.1202E+00 Watts

Label 38, Conductivity: 1.1100E+06 S/m
DC Resistance: 2.1162E-03 Ohms
Current (rms): 4.0466E+01 Amps -3.3709E+01 degrees
Voltage (rms): 2.1302E-01 Volts 1.4739E+02 degrees
Time-avge. loss: 3.4707E+00 Watts

Label 39, Conductivity: 1.1100E+06 S/m
DC Resistance: 2.1162E-03 Ohms
Current (rms): 3.2738E+01 Amps 1.1000E+00 degrees
Voltage (rms): 2.3982E-01 Volts 1.6820E+02 degrees
Time-avge. loss: 2.2768E+00 Watts

Label 40, Conductivity: 1.1100E+06 S/m
DC Resistance: 2.1162E-03 Ohms
Current (rms): 3.1084E+01 Amps 2.0081E+01 degrees
Voltage (rms): 2.5994E-01 Volts -1.7680E+02 degrees
Time-avge. loss: 2.0631E+00 Watts

Label 41, Conductivity: 1.1100E+06 S/m
DC Resistance: 2.1162E-03 Ohms
Current (rms): 3.1093E+01 Amps 1.8980E+01 degrees
Voltage (rms): 2.6645E-01 Volts -1.6546E+02 degrees
Time-avge. loss: 2.0730E+00 Watts

Solver Warning: The solution did not converge within the maximum number of Newton steps.
Time-averaged magnetic energy in the device = 9.74938E-01 Joules
no problems remain to be solved. Solv2d terminates.
Elapsed time 0:38:23

Appendix 12

No load solution with Magnet solver 5.2

```
**************************************************
*                                                *
*                                                *
*                    TH2D                        *
*                                                *
*          The MagNet 2D Eddy Current            *
*           High Order (1-4) Solver              *
*                                                *
*                 Release 5.2                    *
*                                                *
*           Wed Jan 29, 1997  22:11              *
*                                                *
**************************************************
```

```
Maximum mesh size:  5120 nodes, 10240 elements.

Number of problems filed for solution =   1
Problem names:
FMOT
The reordering of the mesh is in progress.

Cartesian (xy) solution.
Polynomial order 1.
Completed pointer generation phase 1.
Completed pointer generation phase 2.
Completed pointer generation phase 3.
Maximum number of field nodes in core =   5120
Maximum number of non-zeros in core =    33280
Number of field nodes =   3804
Number of non-zeros =    15151
Reading CIRCUIT.DAT.

FMOT:  TEST
Frequency:    5.0000E+01 Hz

Matrix Assembly
Manteuffel shift =   .365
newton 1: 526 cg steps; change 100.000%, target .50%; time:3:3
Matrix Assembly
Manteuffel shift =   .365
newton 2: 452 cg steps; change 19.219%, target .50%; time 0:4:54
Matrix Assembly
Manteuffel shift =   .365
newton 3: 457 cg steps; change 6.834%, target .50%; time 0: 6:45
Matrix Assembly
Manteuffel shift =   .365
newton 4: 440 cg steps; change 5.343%, target .50%; time 0: 8:34
Matrix Assembly
Manteuffel shift =   .365
newton 5: 422 cg steps; change 3.524%, target .50%; time 0:10:20
Matrix Assembly
Manteuffel shift =   .365
newton 6: 440 cg steps; change 1.996%, target .50%; time 0:12:15
Matrix Assembly
```

```
Manteuffel shift =   .365
newton 7: 439 cg steps; change 1.501%, target .50%; time 0:14:9
Matrix Assembly
Manteuffel shift =   .365
newton 8: 419 cg steps; change 1.611%, target .50%; time 0:15:58
Matrix Assembly
Manteuffel shift =   .365
newton 9: 439 cg steps; change 1.194%, target .50%; time 0:17:52
Matrix Assembly
Manteuffel shift =   .365
newton 10: 421 cg steps; change 1.073%, target .50%; time 0:19:41
Matrix Assembly
Manteuffel shift =   .365
newton 11: 432 cg steps; change .990%, target .50%; time 0:21:34
Matrix Assembly
Manteuffel shift =   .365
newton 12: 417 cg steps; change .970%, target .50%; time 0:23:24
Matrix Assembly
Manteuffel shift =   .365
newton 13: 440 cg steps; change .903%, target .50%; time 0:25:17
Matrix Assembly
Manteuffel shift =   .365
newton 14: 420 cg steps; change .985%, target .50%; time 0:27:7
Matrix Assembly
Manteuffel shift =   .365
newton 15: 429 cg steps; change .942%, target .50%; time 0:28:59
Matrix Assembly
Manteuffel shift =   .365
newton 16: 421 cg steps; change .983%, target .50%; time 0:30:49
Matrix Assembly
Manteuffel shift =   .365
newton 17: 432 cg steps; change .969%, target .50%; time 0:32:41
Matrix Assembly
Manteuffel shift =   .365
newton 18: 418 cg steps; change .988%, target .50%; time 0:34:30
Matrix Assembly
Manteuffel shift =   .365
newton 19: 442 cg steps; change .973%, target .50%; time 0:36:24
Matrix Assembly
Manteuffel shift =   .365
newton 20: 422 cg steps; change .982%, target .50%; time 0:38:15
Matrix Assembly
Manteuffel shift =   .365
newton 21: 436 cg steps; change .963%, target .50%; time 0:40:13
Matrix Assembly
Manteuffel shift =   .365
newton 22: 420 cg steps; change .964%, target .50%; time 0:42:19
Matrix Assembly
Manteuffel shift =   .365
newton 23: 431 cg steps; change .965%, target .50%; time 0:44:27
Matrix Assembly
Manteuffel shift =   .365
newton 24: 425 cg steps; change .955%, target .50%; time 0:46:24
Matrix Assembly
Manteuffel shift =   .365
newton 25: 422 cg steps; change .979%, target .50%; time 0:48:15
```

```
Matrix Assembly
Manteuffel shift =    .365
newton 26: 423 cg steps; change .974%, target .50%; time 0:50:6
Matrix Assembly
Manteuffel shift =    .365
newton 27: 422 cg steps; change .990%, target .50%; time 0:51:56
Matrix Assembly
Manteuffel shift =    .365
newton 28: 445 cg steps; change 1.019%, target .50%; time 0:53:50
Matrix Assembly
Manteuffel shift =    .365
newton 29: 418 cg steps; change 1.013%, target .50%; time 0:55:40
Matrix Assembly
Manteuffel shift =    .365
newton 30: 423 cg steps; change 1.027%, target .50%; time 0:57:31

Label 1, Conductivity:     4.6000E+07 S/m
         Stranded conductor,       48 turn(s)
         Area of strand:   7.9000E-07 sq. m.
         DC Resistance:    1.0039E-01 Ohms
         Current (rms):    8.7766E+00 Amps    1.4074E+02 degrees
         Voltage (rms):    1.7763E+01 Volts  -1.7760E+02 degrees
         Time-avge. loss:  3.6201E+00 Watts

Label 2, Conductivity:     4.6000E+07 S/
         Stranded conductor,       45 turn(s)
         Area of strand:   7.9000E-07 sq. m.
         DC Resistance:    1.8190E-01 Ohms
         Current (rms):    8.7766E+00 Amps    1.4074E+02 degrees
         Voltage (rms):    1.7307E+01 Volts  -1.7463E+02 degrees
         Time-avge. loss:  6.1495E+00 Watts

Label 3, Conductivity:     4.6000E+07 S/m
         Stranded conductor, 38 turn(s)
         Area of strand:   7.9000E-07 sq. m.
         DC Resistance:    1.5360E-01 Ohms
         Current (rms):    8.7766E+00 Amps    1.4074E+02 degrees
         Voltage (rms):    1.3451E+01 Volts  -1.7061E+02 degrees
         Time-avge. loss:  4.3852E+00 Watts

Label 4, Conductivity:     4.6000E+07 S/m
         Stranded conductor,       29 turn(s)
         Area of strand:   7.9000E-07 sq. m.
         DC Resistance:    1.1722E-01 Ohms
         Current (rms):    8.7766E+00 Amps    1.4074E+02 degrees
         Voltage (rms):    7.4163E+00 Volts  -1.7183E+02 degrees
         Time-avge. loss:  2.5539E+00 Watts

Label 5, Conductivity:     4.6000E+07 S/m
         Stranded conductor,       77 turn(s)
         Area of strand:   3.9600E-07 sq. m.
         DC Resistance:    3.2126E-01 Ohms
         Current (rms):    1.9985E+00 Amps   -1.0981E+02 degrees
         Voltage (rms):    1.1122E+01 Volts  -1.4354E+02 degrees
         Time-avge. loss:  4.8303E-01 Watts
```

```
Label 6, Conductivity:     4.6000E+07 S/m
         Stranded conductor,       83 turn(s)
         Area of strand:   3.9600E-07 sq. m.
         DC Resistance:    3.4629E-01 Ohms
         Current (rms):    1.9985E+00 Amps   -1.0981E+02 degrees
         Voltage (rms):    1.0055E+01 Volts  -9.9097E+01 degrees
         Time-avge. loss:  5.6124E-01 Watts

Label 7, Conductivity:     4.6000E+07 S/m
         Stranded conductor,       83 turn(s)
         Area of strand:   3.9600E-07 sq. m.
         DC Resistance:    3.4629E-01 Ohms
         Current (rms):    1.9985E+00 Amps   -1.0981E+02 degrees
         Voltage (rms):    1.1632E+01 Volts  -7.4617E+01 degrees
         Time-avge. loss:  5.6124E-01 Watts

Label 8 , Conductivity:     4.6000E+07 S/m
          Stranded conductor,       77 turn(s)
          Area of strand:   3.9600E-07 sq. m.
          DC Resistance:    3.2126E-01 Ohms
          Current (rms):    1.9985E+00 Amps   -1.0981E+02 degrees
          Voltage (rms):    1.3625E+01 Volts  -4.7939E+01 degrees
          Time-avge. loss:  4.8303E-01 Watts

Label 9, Conductivity:     4.6000E+07 S/m
         Stranded conductor,       29 turn(s)
         Area of strand:   7.9000E-07 sq. m.
         DC Resistance:    6.0649E-02 Ohms
         Current (rms):    8.7766E+00 Amps   -3.9263E+01 degrees
         Voltage (rms):    7.2107E+00 Volts  -1.9798E+01 degrees
         Time-avge. loss:  1.3214E+00 Watts

Label 10, Conductivity:     4.6000E+07 S/m
          Stranded conductor,       38 turn(s)
          Area of strand:   7.9000E-07 sq. m.
          DC Resistance:    7.9472E-02 Ohms
          Current (rms):    8.7766E+00 Amps   -3.9263E+01 degrees
          Voltage (rms):    1.1814E+01 Volts  -8.7008E+00 degrees
          Time-avge. loss:  2.2688E+00 Watts

Label 11, Conductivity:     4.6000E+07 S/m
          Stranded conductor,       45 turn(s)
          Area of strand:   7.9000E-07 sq. m.
          DC Resistance:    9.4111E-02 Ohms
          Current (rms):    8.7766E+00 Amps   -3.9263E+01 degrees
          Voltage (rms):    1.5716E+01 Volts  -5.8814E+00 degrees
          Time-avge. loss:  3.1817E+00 Watts

Label 12, Conductivity:     4.6000E+07 S/m
          Stranded conductor,       48 turn(s)
          Area of strand:   7.9000E-07 sq. m.
          DC Resistance:    1.0039E-01 Ohms
          Current (rms):    8.7766E+00 Amps   -3.9263E+01 degrees
          Voltage (rms):    1.8389E+01 Volts   2.1719E+00 degrees
          Time-avge. loss:  3.6201E+00 Watts
```

```
Label 13, Conductivity:     4.6000E+07 S/m
          Stranded conductor,       48 turn(s)
          Area of strand:   7.9000E-07 sq. m.
          DC Resistance:    1.0039E-01 Ohms
          Current (rms):   8.7766E+00 Amps   -3.9263E+01 degrees
          Voltage (rms):   1.9906E+01 Volts   8.8981E+00 degrees
          Time-avge. loss:  3.6201E+00 Watts

Label 14, Conductivity:     4.6000E+07 S/m
          Stranded conductor,       45 turn(s)
          Area of strand:   7.9000E-07 sq. m.
          DC Resistance:    9.4111E-02 Ohms
          Current (rms):   8.7766E+00 Amps   -3.9263E+01 degrees
          Voltage (rms):   1.6512E+01 Volts   4.7073E+00 degrees
          Time-avge. loss:  3.1817E+00 Watts

Label 15, Conductivity:     4.6000E+07 S/m
          Stranded conductor,       38 turn(s)
          Area of strand:   7.9000E-07 sq. m.
          DC Resistance:    7.9472E-02 Ohms
          Current (rms):   8.7766E+00 Amps   -3.9263E+01 degrees
          Voltage (rms):   1.1696E+01 Volts   2.8756E+00 degrees
          Time-avge. loss:  2.2689E+00 Watts

Label 16, Conductivity:     4.6000E+07 S/m
          Stranded conductor,       29 turn(s)
          Area of strand:   7.9000E-07 sq. m.
          DC Resistance:    6.0649E-02 Ohms
          Current (rms):   8.7766E+00 Amps   -3.9263E+01 degrees
          Voltage (rms):   7.2228E+00 Volts   1.5791E+01 degrees
          Time-avge. loss:  1.3214E+00 Watts

Label 17, Conductivity:     4.6000E+07 S/m
          Stranded conductor,       77 turn(s)
          Area of strand:   3.9600E-07 sq. m.
          DC Resistance:    3.2126E-01 Ohms
          Current (rms):   1.9985E+00 Amps    7.0192E+01 degrees
          Voltage (rms):   1.1466E+01 Volts   3.4814E+01 degrees
          Time-avge. loss:  4.8303E-01 Watts

Label 18, Conductivity:     4.6000E+07 S/m
          Stranded conductor,       83 turn(s)
          Area of strand:   3.9600E-07 sq. m.
          DC Resistance:    3.4629E-01 Ohms
          Current (rms):   1.9985E+00 Amps    7.0192E+01 degrees
          Voltage (rms):   1.0182E+01 Volts   6.9668E+01 degrees
          Time-avge. loss:  5.6124E-01 Watts

Label 19, Conductivity:     4.6000E+07 S/m
          Stranded conductor,       83 turn(s)
          Area of strand:   3.9600E-07 sq. m.
          DC Resistance:    3.4629E-01 Ohms
          Current (rms):   1.9985E+00 Amps    7.0192E+01 degrees
          Voltage (rms):   1.1987E+01 Volts   1.1060E+02 degrees
          Time-avge. loss:  5.6124E-01 Watts
```

```
Label 20, Conductivity:     4.6000E+07 S/m
          Stranded conductor,       77 turn(s)
          Area of strand:   3.9600E-07 sq. m.
          DC Resistance:    3.2126E-01 Ohms
          Current (rms):   1.9985E+00 Amps   7.0192E+01 degrees
          Voltage (rms):   1.4674E+01 Volts  1.3426E+02 degrees
          Time-avge. loss:  4.8303E-01 Watts

Label 21, Conductivity:     4.6000E+07 S/m
          Stranded conductor,       29 turn(s)
          Area of strand:   7.9000E-07 sq. m.
          DC Resistance:    6.0649E-02 Ohms
          Current (rms):   8.7766E+00 Amps   1.4074E+02 degrees
          Voltage (rms):   6.9562E+00 Volts  1.5491E+02 degrees
          Time-avge. loss:  1.3214E+00 Watts

Label 22, Conductivity:     4.6000E+07 S/m
          Stranded conductor,       38 turn(s)
          Area of strand:   7.9000E-07 sq. m.
          DC Resistance:    7.9472E-02 Ohms
          Current (rms):   8.7766E+00 Amps   1.4074E+02 degrees
          Voltage (rms):   1.2033E+01 Volts  1.6804E+02 degrees
          Time-avge. loss:  2.2688E+00 Watts

Label 23, Conductivity:     4.6000E+07 S/m
          Stranded conductor,       45 turn(s)
          Area of strand:   7.9000E-07 sq. m.
          DC Resistance:    9.4111E-02 Ohms
          Current (rms):   8.7766E+00 Amps   1.4074E+02 degrees
          Voltage (rms):   1.7051E+01 Volts -1.7862E+02 degrees
          Time-avge. loss:  3.1817E+00 Watts

Label 24, Conductivity:     4.6000E+07 S/m
          Stranded conductor,       48 turn(s)
          Area of strand:   7.9000E-07 sq. m.
          DC Resistance:    1.0039E-01 Ohms
          Current (rms):   8.7766E+00 Amps   1.4074E+02 degrees
          Voltage (rms):   1.8711E+01 Volts -1.7679E+02 degrees
          Time-avge. loss:  3.6201E+00 Watts

Label 25, Conductivity:     2.3800E+07 S/m
          DC Resistance:    9.8698E-05 Ohms
          Current (rms):   4.0792E+02 Amps   1.0002E+01 degrees
          Voltage (rms):   2.8825E-01 Volts  1.7810E+02 degrees
          Time-avge. loss:  1.6962E+01 Watts

Label 26, Conductivity:     2.3800E+07 S/m
          DC Resistance:    9.8698E-05 Ohms
          Current (rms):   4.4358E+02 Amps  -1.0332E+01 degrees
          Voltage (rms):   2.6117E-01 Volts -1.7782E+02 degrees
          Time-avge. loss:  1.9708E+01 Watts

Label 27, Conductivity:     2.3800E+07 S/m
          DC Resistance:    9.8698E-05 Ohms
          Current (rms):   3.2811E+02 Amps  -7.6116E+00 degrees
          Voltage (rms):   1.9911E-01 Volts -1.6919E+02 degrees
```

```
          Time-avge. loss:  1.0708E+01 Watts

Label 28, Conductivity:     2.3800E+07 S/m
          DC Resistance:    9.8698E-05 Ohms
          Current (rms):   9.4655E+01 Amps    3.8423E+01 degrees
          Voltage (rms):   1.2262E-01 Volts  -1.4581E+02 degrees
          Time-avge. loss:  8.9116E-01 Watts

Label 29, Conductivity:     2.3800E+07 S/m
          DC Resistance:    9.8698E-05 Ohms
          Current (rms):   2.4203E+02 Amps    8.5338E+01 degrees
          Voltage (rms):   9.5902E-02 Volts  -9.1247E+01 degrees
          Time-avge. loss:  5.8258E+00 Watts

Label 30, Conductivity:     2.3800E+07 S/m
          DC Resistance:    9.8698E-05 Ohms
          Current (rms):   2.5000E+02 Amps    1.0443E+02 degrees
          Voltage (rms):   1.4156E-01 Volts  -4.5566E+01 degrees
          Time-avge. loss:  6.2150E+00 Watts

Label 31, Conductivity:     2.3800E+07 S/m
          DC Resistance:    9.8697E-05 Ohms
          Current (rms):   3.8300E+02 Amps    1.5478E+02 degrees
          Voltage (rms):   2.1379E-01 Volts  -2.3441E+01 degrees
          Time-avge. loss:  1.4582E+01 Watts

Label 32, Conductivity:     2.3800E+07 S/m
          DC Resistance:    9.8698E-05 Ohms
          Current (rms):   4.5107E+02 Amps    1.7886E+02 degrees
          Voltage (rms):   2.6801E-01 Volts  -1.1746E+01 degrees
          Time-avge. loss:  2.0379E+01 Watts

Label 33, Conductivity:     2.3800E+07 S/m
          DC Resistance:    9.8698E-05 Ohms
          Current (rms):   4.4454E+02 Amps   -1.6600E+02 degrees
          Voltage (rms):   2.9018E-01 Volts  -4.6509E+00 degrees
          Time-avge. loss:  2.0113E+01 Watts

Label 34, Conductivity:     2.3800E+07 S/m
          DC Resistance:    9.8698E-05 Ohms
          Current (rms):   4.2656E+02 Amps   -1.7696E+02 degrees
          Voltage (rms):   2.7915E-01 Volts  -5.9822E-01 degrees
          Time-avge. loss:  1.8416E+01 Watts

Label 35, Conductivity:     2.3800E+07 S/m
          DC Resistance:    9.8698E-05 Ohms
          Current (rms):   4.3432E+02 Amps    1.5764E+02 degrees
          Voltage (rms):   2.3287E-01 Volts   3.7311E+00 degrees
          Time-avge. loss:  1.8780E+01 Watts

Label 36, Conductivity:     2.3800E+07 S/m
          DC Resistance:    9.8697E-05 Ohms
          Current (rms):   1.8130E+02 Amps   -1.7723E+02 degrees
          Voltage (rms):   1.5797E-01 Volts   1.8273E+01 degrees
          Time-avge. loss:  3.2696E+00 Watts
```

```
Label 37, Conductivity:     2.3800E+07 S/m
          DC Resistance:    9.8698E-05 Ohms
          Current (rms):   1.9985E+02 Amps   -1.0165E+02 degrees
          Voltage (rms):   9.8438E-02 Volts   5.7728E+01 degrees
          Time-avge. loss:  3.9723E+00 Watts

Label 38, Conductivity:     2.3800E+07 S/m
          DC Resistance:    9.8698E-05 Ohms
          Current (rms):   2.4166E+02 Amps   -9.6692E+01 degrees
          Voltage (rms):   1.1011E-01 Volts   1.1560E+02 degrees
          Time-avge. loss:  5.8066E+00 Watts

Label 39, Conductivity:     2.3800E+07 S/m
          DC Resistance:    9.8698E-05 Ohms
          Current (rms):   3.1399E+02 Amps   -4.4537E+01 degrees
          Voltage (rms):   1.7855E-01 Volts   1.4809E+02 degrees
          Time-avge. loss:  9.8048E+00 Watts

Label 40, Conductivity:     2.3800E+07 S/m
          DC Resistance:    9.8698E-05 Ohms
          Current (rms):   4.5862E+02 Amps   -1.3602E+01 degrees
          Voltage (rms):   2.4632E-01 Volts   1.6348E+02 degrees
          Time-avge. loss:  2.0938E+01 Watts

Label 41, Conductivity:     2.3800E+07 S/m
          DC Resistance:    9.8699E-05 Ohms
          Current (rms):   4.4792E+02 Amps    9.6956E+00 degrees
          Voltage (rms):   2.8346E-01 Volts   1.7270E+02 degrees
          Time-avge. loss:  2.0290E+01 Watts

Solver Warning: The solution did not converge within the maximum
number of Newton steps.

Time-averaged magnetic energy in the device =  9.48607E-01 Joules

No problems remain to be solved. Solv2d terminates.

Elapsed time  0:58: 6
```

Appendix 13

List of important formulas for biological effects on living organisms due to electromagnetic fields

Amperes circuital relationship

$$B = \frac{\mu_0 I}{2\pi r} \quad (1)$$

where,

I = current in the conductor (wire) in amperes,
r = radial distance from the conductor to the point in meters
$\mu = 4\pi x 10^{-7}$ henry per meter, (permittivity of free space)
B = magnetic flux density in Tesla

Faraday's law,

$$E = \frac{\omega BR}{2} \quad (2)$$

where,

ώ = frequency of the alternating field in radians per second
B = flux density in tesla
R = radius of circular path

Lorentz's equation

$$F = J \times B \quad (3)$$

$$J = \sigma E \quad (4)$$

where,

F = Lorentz's force exerted on each volume of conducting medium
J = electric current density
B = flux density in tesla
E = electric field density in volts per meter
σ = conductivity in siemens per meter

Explanation:
When a conducting fluid medium flows in a region in which there are orthogonal electric (E) and magnetic (B) fields, the Lorentz's force is given by equation (3).

The five Maxwell equations are:

$$\nabla \times E = -j\omega\mu_0 H \tag{5}$$

$$\nabla \times H = j\omega\epsilon_0 E + J \tag{6}$$

$$\nabla \cdot D = \rho \tag{7}$$

$$\nabla \cdot J = -j\omega\rho \tag{8}$$

$$\nabla \cdot B = 0 \tag{9}$$

[Malmivuo, 1995].
Equation (5) is a statement of Faraday's law that time varying magnetic field H induces an electric field E
Equation (6) is a statement of Ampere's law, that the line integral of magnetic field H around a closed loop equals the total current in the loop.
Equation (7) arises from Coulombs law and relates the electric displacement D to the sources that generate it namely the charge density ρ
Equation (8) is a statement of conservation of charge, namely that its outflow from any closed region (evaluated from $\nabla \cdot$) can arise only if the charge contained is depleted
Equation (9) recognizes that no magnetic charges exist, and hence the magnetic induction, must be solenoidal.

Brief review of basic Electromagnetics [Jin, J., The finite element method in Electromagnetics, pp. 1-10]

The problem of electromagnetic analysis is actually a problem of solving Maxwell's equations subject to given boundary conditions. Books of electromagnetic theory can be consulted.

Maxwell's equations are a set of fundamental equations governing all macroscopic electromagnetic phenomena. They can be written in both differential and integral form, but they will be presented here in differential form since they lead to differential equations to be dealt with by the finite element method.

The General Differential Form

For general time varying fields, Maxwell's equations in differential form can be written as

$$\nabla \times E + \frac{\partial B}{\partial t} = 0 \quad (Faraday's\ law) \tag{10}$$

$$\nabla \times H - \frac{\partial D}{\partial t} = J \quad (Maxwell\text{-}Ampere\ law) \tag{11}$$

$$\nabla \cdot \boldsymbol{D} = \rho \quad (\textit{Gauss's law}) \tag{12}$$

$$\nabla \cdot \boldsymbol{B} = 0 \ (\textit{Gauss's law magnetic}) \tag{13}$$

where,

E = electric field intensity (volts per meter)
D = electric flux density (coulombs per meter^2)
H = magnetic field intensity (amperes per meter)
B = magnetic flux density (webers per meter^2)
J = electric current density (amperes per meter^2)
ρ = electric charge density (coulombs per meter^3).

Another fundamental equation known as the equation of continuity can be written as

$$\nabla \cdot \boldsymbol{J} = -\frac{\partial \rho}{\partial t} \ (\textit{equation of continuity}) \tag{14}$$

which specifies the conservation of charge.
Equations (10) to (12) or (10), (11) and (15) can be chosen as independent equations. The other two, (13) and (14) or (12) and (13) can be derived from the independent equations, and are thus called auxiliary equations.

Electro and Magnetostatic fields

If the fields do not vary with time, the fields are static the differential terms in Equations (10) to (14) disappear and the equations can be rewritten as

$$\nabla \times \boldsymbol{E} = 0 \tag{15}$$

$$\nabla \times \boldsymbol{H} = \boldsymbol{J} \tag{16}$$

$$\nabla \cdot \boldsymbol{J} = 0 \tag{17}$$

whereas (12) and (13) remain the same. This means when the fields are static, electric or magnetic, , there is no interaction. The electric field can be described by (12) and (15) and the magnetic field is described by (13) and (16)and (17) being a natural consequence of (16).

Time Harmonic Fields

When the field quantities in Maxwell's equations are harmonically oscillating functions with a single frequency, we have a time harmonic field. Using complex phaser notation, equation (10), (11) and (14) can be written in a specified form as,

$$\nabla \times \boldsymbol{E} + j\omega \boldsymbol{B} = 0 \tag{18}$$

where the time convention $e^{j\acute{\omega}t}$ is used and suppressed, and ώ is angular frequency. From the equations above, it is evident that in this case the electric and magnetic fields exist

$$\nabla \times H - j\omega D = J \tag{19}$$

$$\nabla \cdot J = -j\omega\rho \tag{20}$$

simultaneously (they coexist), and they interact with each other, and it is also evident that the static case is the limiting case of the harmonic fields as the frequency ώ approaches zero.

Constitutive Relations

The three independent equations among the five Maxwell equations described above are in indefinite form since the number of equations is less than the number of unknowns. Maxwell equations become definitive when the constitutive relations between the field quantities are specified. The constitutive relations describe the macroscopic properties of the medium being considered. For a simple medium they are

$$D = \epsilon E \tag{21}$$

$$B = \mu H \tag{22}$$

$$J = \sigma E \tag{23}$$

Where the constitutive parameters, ε, μ and σ denote respectively, the permitivity (farads per meter), permeability (henrys per meter), and conductivity (Siemens per meter) of the medium. These parameters are tensors for anisotropic media, and scalars for isotropic media. For inhomogeneous media, they are functions of position, while for homogeneous media they are not.

Induced currents in human tissue

Equations (1), (2), (3) and (4) explain how current can be induced a volume due to fields across it. The permeability of human tissue is homogeneous but close to that of air. From Equations (15), (16) and (17) indicate that there can not be induced currents if the field is not varying with time. However, there will be Lorentz's forces in the tissue involved from Equation (3). The effects can be found in biomagnetic studies [Malmivuo 1995].

It can also be shown that at the power frequency there can never be radiation effects due to the currents flowing in the conductors including in the motor to a person near to them [Polk, 1986]. There can only be induced currents in the person if he/she is too near due to the magnetic field. The magnetic field at extra low frequencies is only dependent on the current that is flowing in the conductor at that moment [Polk, 1986].

Appendix 14 CENELEC extract: prENV 50166-1:1994
Basic restrictions on induced current density and contact current

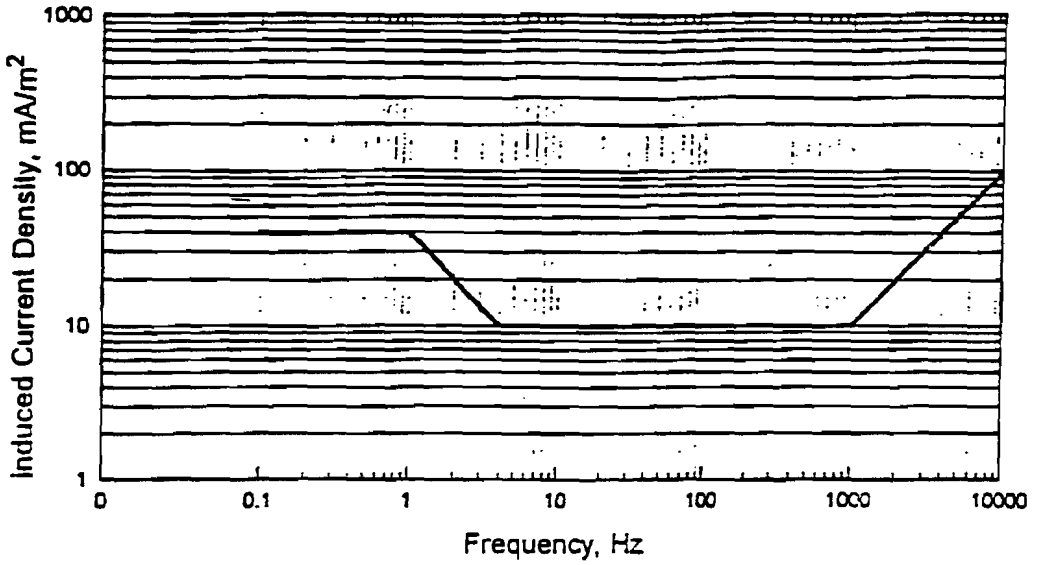

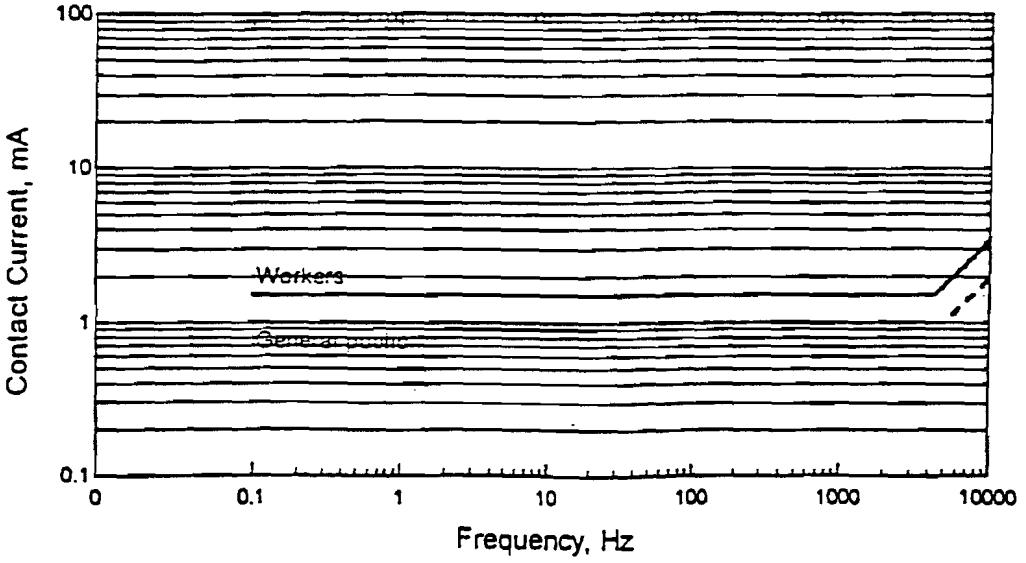

Appendix 15 CENELEC extract: prENV 50166-1:1994
Electric and magnetic field levels

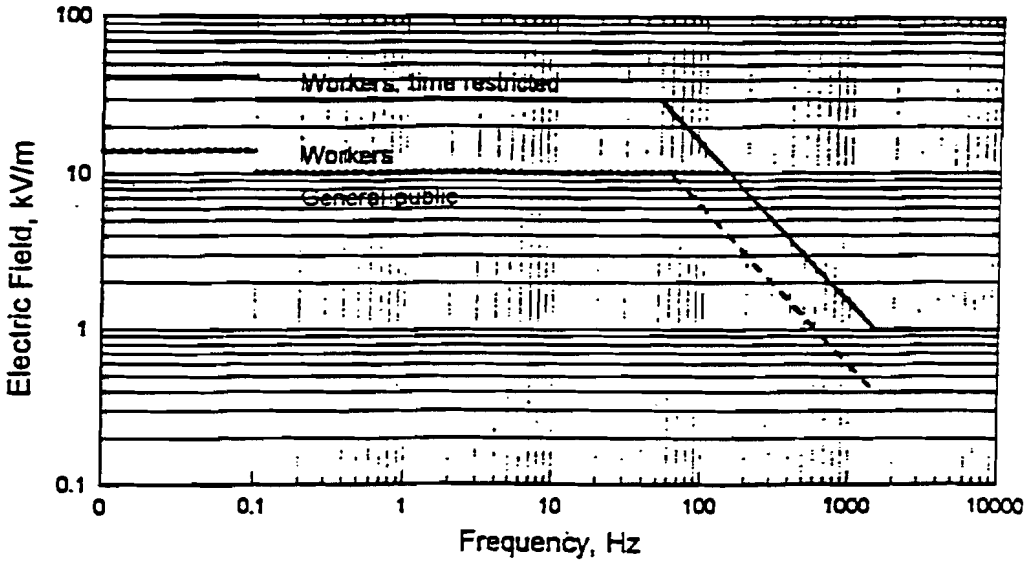

Version B

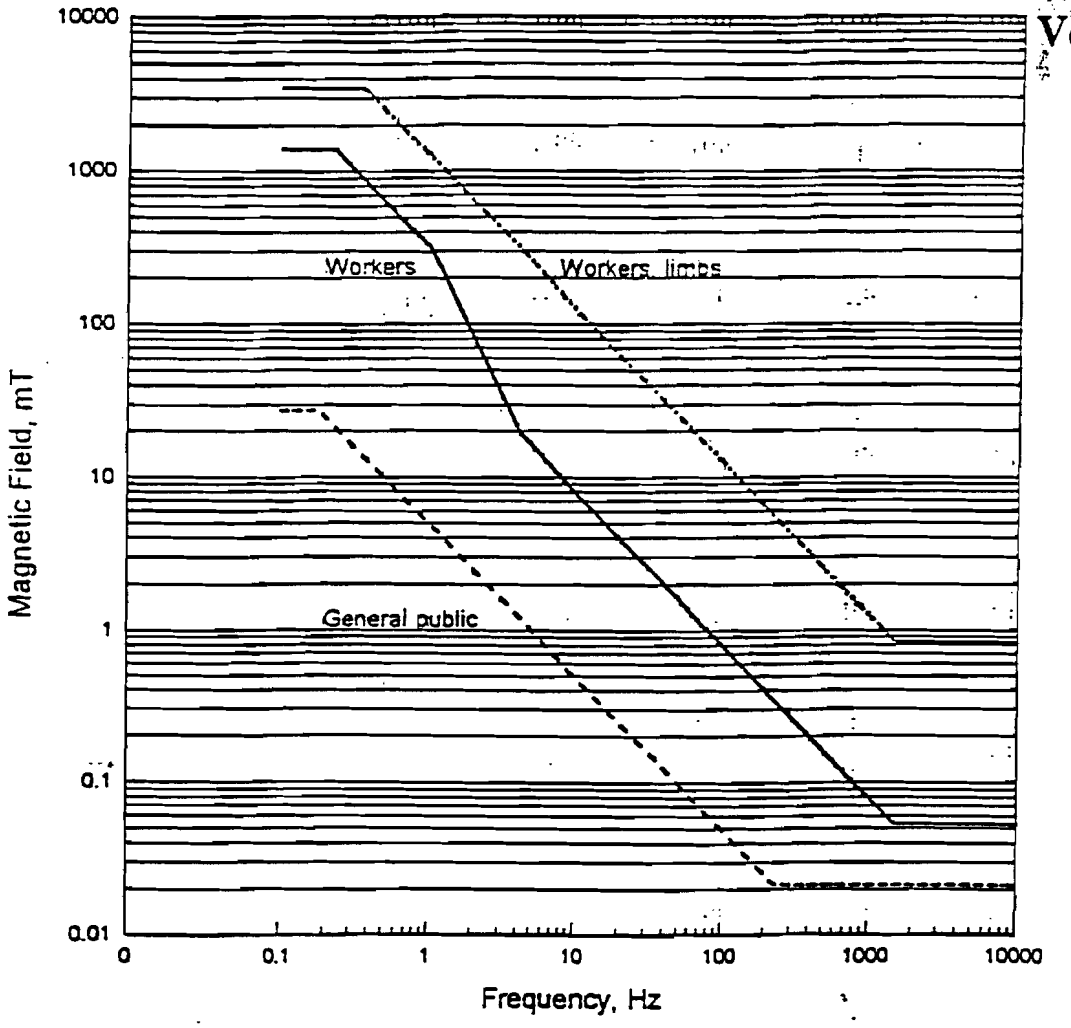

Appendix 16

SIMULATION MODEL FOR A CAPACITOR SINGLE PHASE INDUCTION MOTOR

Brief explanation of the terms used in the model

Rsa = 3.89 ohms; resistance of the main winding
Rsb = 6.34 ohms; resistance of the auxiliary winding
Rr = 4.52 ohms; rotor resistance referred to the main winding
Lsiga = 30e-3 henrys; leakage inductance of the main winding
Lsigb = 50e-3 henrys; leakage inductance of the auxiliary winding
Lm = 0.45 henrys; magnetizing inductance
C = 25e-6F; value of capacitor for the auxiliary winding
J = 11e-4 kgm^2; inertia of the rotating parts
F = 50 Hz; supply frequency
Upeak = 240*sqrt(2); amplitude of the supply voltage
xi = INTMOD(2*pi*F);
Usup = Upeak*cos(xi); instantaneous voltage of the supply
Ucap = voltage across the capacitor
Uaux = Upeak*sin(-xi); voltage across the auxiliary winding
Uaux = Usup-Ucap;
Fssa = INT(Usup-Rsa*Issa); flux due to the main winding
Fssb = INT(Uaux-Rsb*Issb); flux due to the auxiliary winding
Issa = (Fssa-Frsa)/Lsiga; current in the main winding
Issb = (Fssb-Frsb)/Lsigb; current in the auxiliary winding
Ucap = INT(Issb/C);
Isra = cos(theta)*Issa + sin(theta)*Issb; rotor current due to the current in the main winding
Isrb = -sin(theta)*Issa + cos(theta)*Issb; rotor current due to the current in the auxiliary winding
Frra = INT(Rr*(-Frra/Lm+Isra)); flux in the air gap due to the current in the main winding
Frrb = INT(Rr*(-Frrb/Lm+Isrb)); flux in the air gap due to the current in the auxiliary winding
Frsa = cos(theta)*Frra - sin(theta)*Frrb; stator flux due to the current in the main winding
Frsb = sin(theta)*Frra + cos(theta)*Frrb; stator flux due to the current in the auxiliary winding
Torque = -Issa*Fssb+Issb*Fssa; torque developed Nm
Speed = INT((Torque-Load)/J); shaft speed in rad/sec
Shaftspeed = Speed/(2*pi);
Shafttorque = Torque;
theta = INTMOD(Speed);
Load = ABS(Speed)*Speed*3/(310^2); A fan load is proportional to the square of the shaft speed
fluxs = sqrt(fssa^2 + fssb^2); resultant stator flux
fluxr = sqrt(frra^2 + frrb^2); resultant air gap flux

Appendix 16 (cont.)

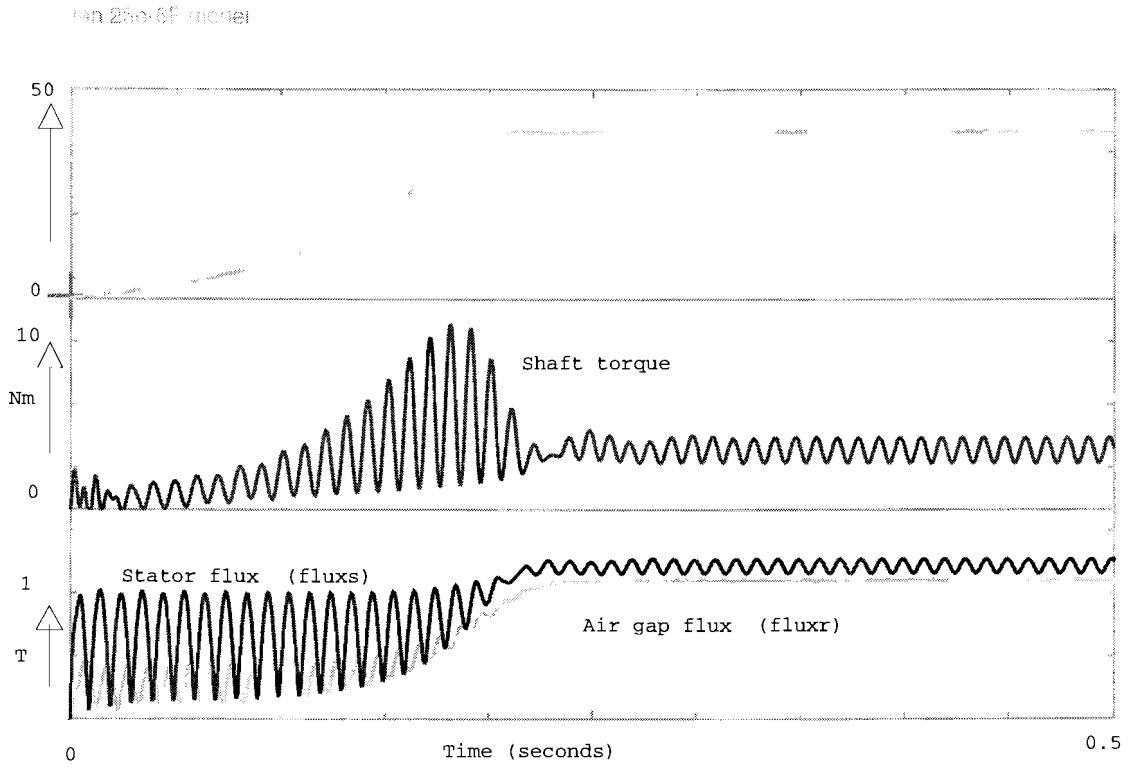

Fig. 16.1 Simulation model for a capacitor single phase induction motor (optimized condition)

The top graph in Fig. 16.1 is the speed in radians per second versus time in seconds. The middle one is the shaft torque versus time. The lower one is the stator flux and the air gap flux. The simulation of the capacitor single phase induction motor has been done for a fan load such as a blower.

The shaft speed is smooth at only one load point. By simulation in general it was found that, if the load is changed to say twice, the shaft speed vibrates, the torque ripple increases, the air gap flux (fluxr) reduces and is no longer smooth. This is concluded by Vandenput [Vandenput, 1985]. In the optimized condition the air gap flux was also circular.

As the load is increased the air gap flux (fluxr) diminishes and pulsates. The stator current also increases. From this result and the conclusions from Smith [Smith, 1990] and Ho [Ho et al, 1995], the stray field around the motor increases as stated in section 1.2.

SHIRIMA.PCX